

UC Riverside

UC Riverside Electronic Theses and Dissertations

Title

Evaluating the Changing Mass Spectra Signature and Secondary Impact of Emissions Generated by Charbroiling Beef Hamburger Patties Using Data from Environmental Chamber and Oxidation Flow Reactor Experiments

Permalink

<https://escholarship.org/uc/item/1tw2p8rg>

Author

Bergeson, Miles Alan

Publication Date

2018

Copyright Information

This work is made available under the terms of a Creative Commons Attribution License, available at <https://creativecommons.org/licenses/by/4.0/>

Peer reviewed|Thesis/dissertation

UNIVERSITY OF CALIFORNIA
RIVERSIDE

Evaluating the Changing Mass Spectra Signature and Secondary Impact of Emissions
Generated by Charbroiling Beef Hamburger Patties Using Data from Environmental
Chamber and Oxidation Flow Reactor Experiments

A Thesis submitted in partial satisfaction
of the requirements for the degree of

Master of Science

in

Chemical and Environmental Engineering

by

Miles Alann Bergeson

December 2018

Thesis Committee:

Dr. David R. Cocker III, Chairperson

Dr. Kelley Barsanti

Dr. Don Collins

Copyright by
Miles Alann Bergeson
2018

The Thesis of Miles Alann Bergeson is approved:

Committee Chairperson

University of California, Riverside

Acknowledgements

First and foremost, I would like to thank Dr. David Cocker for his kind and thoughtful mentoring throughout the duration of my graduate work, and for his expert guidance over the course of this research. I would also like to thank Dr. Kelley Barsanti and Dr. Don Collins for their involvement with my research and for agreeing to be a part of my Thesis Committee. I am grateful for the assistance of my fellow researchers and their aid from the very start of my research. Without their help and expertise none of this would have been possible. Special thanks to Lenny Apontti for his endless support, Paul Van Rooy for his assistance with the environmental chamber, and to Ayla Moretti for her assistance with the oxidation flow reactor. I appreciate the support of Dean Simkins, and his encouragement to pursue my master's degree in the first place. I am thankful for the patience and support of my family during these long two years. And last, I am eternally grateful for my wider group of friends, who without their support I would have never made it this far.

ABSTRACT OF THE THESIS

Evaluating the Changing Mass Spectra Signature and Secondary Impact of Emissions Generated by Charbroiling Beef Hamburger Patties Using Data from Environmental Chamber and Oxidation Flow Reactor Experiments

by

Miles Alann Bergeson

Master of Science, Chemical and Environmental Engineering
University of California, Riverside, December 2018
Dr. David Cocker, Chairperson

Commercial cooking emissions are a growing concern in regions like the South Coast Air Basin, and while extensive research has been conducted to evaluate the primary emissions from this source, limited research has been conducted regarding the formation of secondary organic aerosol (SOA) from this source. The research for this thesis used an environmental chamber and an oxidation flow reactor (OFR) to evaluate the emissions generated by beef hamburger charbroiling, already established as the cooking method and meat type that predominantly contributes to commercial cooking emissions. For unfiltered environmental chamber experiments, representing both the primary organic aerosol (POA) and SOA created by this source, the %SOA production evolved from $13 \pm 5.6\%$ to $24 \pm 6.7\%$ over four hours while the %SOA for the filtered environmental chamber experiments, representing only SOA produced from gaseous

emissions of this source, remained relatively stable at $90 \pm 9.8\%$ on average. Using the results from the OFR with data from the environmental chamber experiments, linear combination of variables was used to find 57% SOA production for the unfiltered emissions. Additionally, the mass spectra for these experiments were evaluated and a significant change in character was observed from start to finish of the environmental chamber experiments and between individual experiment types, showing an increased oxidation and a shift towards smaller organic ions with increasing atmospheric exposure. Angle theta was used to quantify this change. From start to finish, a change of $19.3 \pm 2.6^\circ$ was observed for the unfiltered environmental chamber experiments and a change of $51.8 \pm 3.5^\circ$ was observed between the start and the finish of the filtered chamber experiments. This supports the finding that SOA from meat charbroiling is far more ready to participate in atmospheric chemistry than POA emissions. Comparing the OFR spectrum to the initial unfiltered and final filtered spectra respectively yielded an angle theta of $46.2 \pm 0.9^\circ$ and $19.3 \pm 4.4^\circ$. Altogether, the early findings from this research show that the secondary impact of commercial cooking emissions has significantly been underestimated in previous research and that this emission source has a far greater SOA forming potential than suspected.

Table of Contents

Acknowledgements

Abstract

1. Introduction.....	1
2. Environmental Chamber Evaluation of Meat Charbroiling Emissions	11
2.1 Introduction	11
2.2 Experimental Methods	13
2.2.1 <i>Sampling Methodology</i>	13
2.2.2 <i>Instrumental Analysis</i>	15
2.2.3 <i>Data Analysis</i>	16
2.3 Results and Discussion.....	16
2.3.1 <i>Evaluating the Primary Organic Aerosol Emissions</i>	16
2.3.2 <i>Mechanism of Emission Aging</i>	18
2.3.3 <i>Character Change of Aging Emissions</i>	22
2.3.4 <i>Percent Secondary Organic Aerosol Production</i>	26
2.4 Summary	28
2.5 References	32
3. Oxidation Flow Reactor Evaluation of Meat Charbroiling Emissions	35
3.1 Introduction	35
3.2 Experimental Methods	38
3.2.1 <i>Sampling Methodology</i>	38
3.2.2 <i>Instrumental Analysis</i>	40

3.2.3 <i>Data Analysis</i>	41
3.3 Results and Discussion.....	41
3.3.1 <i>Aging in Oxidation Flow Reactor Experiment</i>	41
3.3.2 <i>Character Change in Oxidation Flow Reactor Experiment</i>	44
3.3.3 <i>Percent Secondary Organic Aerosol Production</i>	49
3.4 Summary	50
3.5 References	53
4. Conclusion	56

List of Figures

2.1 Schematic of dilution sampling set-up.....	14
2.2 Normalized average mass spectrum of primary hamburger charbroiling emissions	18
2.3 Representative triangle plots for environmental chamber experiments.....	20
2.4 Representative Van Krevelen diagrams for environmental chamber experiments.....	21
2.5 Mass spectra comparison between start and finish of environmental chamber experiments	23
2.6 Mass spectra comparison of organic and inorganic ions for environmental chamber experiments	25
2.7 Percent secondary organic aerosol production for environmental chamber experiments	27
3.1 Schematic of oxidation flow reactor set-up	40
3.2 Triangle plot comparison between environmental chamber and oxidation flow reactor experiments	42
3.3 Van Krevelen diagram comparison between environmental chamber and oxidation flow reactor experiments.....	44
3.4 Mass spectra comparison between environmental chamber and oxidation flow reactor experiments	45
3.5 Mass spectra comparison of organic and inorganic ions for environmental chamber and oxidation flow reactor experiments.....	48

List of Tables

2.1 High resolution analysis of three ions for environmental chamber experiments.....	24
3.1 High resolution analysis of three ions for environmental chamber and oxidation flow reactor experiments.....	46
3.2 Values used in linear combination of variables for percent secondary organic aerosol calculation.....	50

Chapter 1

Introduction

Emissions from commercial cooking operations have been an air quality concern since the late 1990's when the South Coast Air Quality Management District (SCAQMD) implemented control standards for chain-driven charbroilers in commercial cooking facilities. The South Coast Air Basin, which is responsible for much of the greater Los Angeles urban area, was the only region at the time with documented regulations in place for particulate matter (PM) emissions from commercial cooking sources (Roe *et al.*, 2002). Since then, primary emissions from commercial cooking operations have become the single greatest source of fine particulate matter (PM_{2.5}) in the South Coast Air Basin, greater even than the primary PM_{2.5} emissions from heavy-duty diesel trucks or passenger cars (AQMD, 2016). In 2012, the annual average of PM_{2.5} emissions from commercial cooking was estimated at 10.4 tons per day and represented 72% of the emissions from this source category (AQMD, 2016). This same report projects that this number will rise to 12.8 tons per day by 2031. As of 2016, SCAQMD has put further regulations in place for commercial cooking sources with the aim of reducing the total annual average of PM_{2.5} emitted from this source daily by 3.3 tons by 2025 (AQMD, 2016).

Underfired charbroiling of meat has since been isolated as the cooking method responsible for contributing the most to primary emissions from commercial cooking sources (Rogge *et al.*, 1991). An underfired charbroiler is a cooking device that utilizes an open flame below a grate to cook food and can be used both commercially and residentially. The residential version of the underfired charbroiler is often referred to as a

barbeque grill. Total PM_{2.5} emission rates for charbroiled meat range from 4.4 to 11.6 grams per kilogram of uncooked meat (McDonald *et al.*, 2003). Charbroiling emissions have also been found to produce the greatest concentration of volatile organic compounds (VOCs) compared to other cooking methods (Wang *et al.*, 2017). These emissions were found to be composed predominantly of alkanes, which are thought to be produced by the incomplete combustion of fats from the meats cooked (Hildemann *et al.*, 1994; Rogge *et al.*, 1991).

The emission rates vary within this range depending on the type of meat cooked, though studies have consistently found increasing emissions with increasing fat content (Hildemann *et al.*, 1994; McDonald *et al.*, 2003; Mohr *et al.*, 2003). Fatty meats and underfired charbroilers make such a potent pairing due to the charbroiler's open flame and high cooking temperature. This unique set-up allows liquid fat droplets released from the meat during cooking to drip down into the open flame where the fat droplets can become volatilized and entrained in the exhaust fume (Rogge *et al.*, 1991). Due to the nature of this process, PM_{2.5} is the dominant fraction of PM₁₀ emitted by commercial cooking methods (Zhao *et al.*, 2007). PM_{2.5}, or fine PM, is defined as PM with an aerodynamic diameter equal to or less than 2.5 microns. Similarly, PM₁₀ is often referred to as coarse PM and is defined as PM with an aerodynamic diameter equal to or less than 10 microns.

Both categories of PM pollution, PM_{2.5} and PM₁₀, have serious implications for a wide range of environmental and health concerns. PM_{2.5} is the main cause of reduced visibility in urban and natural areas and can also contribute to acidification of soil or

water, shifting the nutrient value of agricultural fields or bodies of water, and the discoloration of buildings and monuments. Exposure to PM pollution also affects human and animal health, especially concerning heart and lung health. A close relationship between airborne PM and increased morbidity and mortality of respiratory and cardiovascular diseases have been established using epidemiological and experimental evidence (Araujo and Nel, 2009; Breysse *et al.*, 2013; Kelly and Fussell, 2011; Li *et al.*, 2012; Pelucchi *et al.*, 2009; Shah *et al.*, 2013). Furthermore, many studies have found associations between PM pollution with decreased lung function, increased respiratory symptoms, asthma exacerbations, increased medication use, and increased hospital admissions (BéruBé *et al.*, 2007; Kreyling *et al.*, 2006; Utell and Frampton, 2000).

A portion of why PM pollution has a negative effect on human health stems from small particle size, as a smaller particle can travel deeper into the lungs and even enter the bloodstream. Fine particles have also been found to be more biologically active than larger particles due to their greater surface area per mass (Oberdörster *et al.*, 2005). The chemical composition of PM pollution has been found to pose an additional health risk as well. McDonald *et al.* (2003) reported that charbroiling was especially efficient at producing polycyclic aromatic hydrocarbons (PAHs) compared to other cooking methods, and that hamburgers are more efficient at producing PAHs than other meat type. These PAH compounds are classified as a hazardous air pollutant by the U.S. Environmental Protection Agency (EPA), and several PAH compounds that are found in charbroiling emissions are also associated with the adverse health effects of well-studied diesel exhaust emissions (Li *et al.*, 2014). Furthermore, aldehydes are also frequently

observed in charbroiling cooking emissions and pose a significant health risk as well (Gysel *et al.*, 2016; Klein *et al.*, 2016; Schauer *et al.*, 1999). For example, formaldehyde and acetaldehyde are both classified as carcinogens (IARC, 2006) and have both been found in the emissions of commercial meat cooking operations (Gysel *et al.*, 2017). Altogether, Li *et al.* (2014) found that the cellular responses to cooking emissions and their potential mechanisms resembled those associated with traffic-derived emissions, suggesting that the organic fractions emitted from commercial-grade charbroiling meat operations may pose environmental and occupational health hazards that put those exposed at a greater health risk in a similar way that exposure to traffic-derived emissions pose a heightened health risk.

Thus far, the primary emissions from meat charbroiling have been well-documented in previous literature. Primary emissions are the particulate and gaseous emissions that are initially generated by an emission source. These primary emissions often react under atmospheric conditions and go on to participate in ozone formation, condense onto existing particles, or nucleate to form new particles. When primary emissions behave in this manner, the new gases and aerosols produced through this atmospheric chemistry are referred to as the secondary emissions or the secondary effects of an emission source. Specifically, aerosol formed by primary emissions that react with sunlight, hydroxyl radicals, or other airborne chemicals is referred to as secondary organic aerosol (SOA). This SOA formation is a major contributor to the PM_{2.5} that is suspended in the atmosphere, which in turn affects climate, visibility, and again, human health.

The secondary effects of emissions can also include the formation of ozone. Cheng *et al.* (2016) found that charbroiling meat had the highest ozone forming potential (OFP) of all tested cooking methods, with 4.81 grams of ozone produced per gram of VOC emitted ($\text{g O}_3/\text{g VOC}$). Furthermore, Cheng *et al.* (2016) found that alkenes mainly contributed to this potential. The OFP is used to classify compounds according to their ability to form ozone and is defined as the change in the amount of ozone formed due to a change in emissions of that compound (Derwent and Jenkin, 1991; Derwent *et al.*, 1996, 1998). For context, the OFP for charbroiling meat is greater than the OFP of emissions produced by gas stations ($4.67 \text{ g O}_3/\text{g VOC}$) and coal-fired power plants ($3.46 \text{ g O}_3/\text{g VOC}$), though less than the emissions produced by furniture painting ($5.89 \text{ g O}_3/\text{g VOC}$) and automobile painting ($5.59 \text{ g O}_3/\text{g VOC}$) (Cheng *et al.*, 2016).

The sources of SOA have traditionally been difficult to predict and impossible to directly measure due to the complicated and non-linear formation pathway of SOA. For example, VOCs can evaporate from primary PM and participate in the ozone cycle, compounds unrelated to the emissions source can condense onto the primary PM produced by that source, or VOCs from a source can enter the atmosphere as gases where they react with other existing gases to form new aerosol. Additionally, both Donahue *et al.* (2006) and Jimenez *et al.* (2009) have demonstrated that the oxidation of VOCs evaporated from primary PM can produce significant SOA. This suggests that commercial cooking emissions, already a leading source of primary PM pollution in the South Coast Air Basin, could be contributing immensely to the SOA generation in the same region. Hayes *et al.* (2010) was able to estimate that cooking emissions contributed

19-35% of SOA mass in downtown Los Angeles during the California Research at the Nexus of Air Quality and Climate Change (CalNex). However, the computer model that generated this estimate used the same parameters as vehicle exhaust due to the lack of specific information regarding the SOA formation from cooking emissions. In stark contrast to the previous research on primary emissions generated by meat charbroiling emissions, very little research has been completed thus far to establish the secondary impact generated by this emission source.

The research for this thesis was conducted with the intent to contribute to the limited understanding of the secondary emissions from meat charbroiling. This includes characterizing the emissions as they age and developing a percent estimation for the SOA generation of this source. Chamber experiments were conducted inside the Atmospheric Process Laboratory (APL) at the College of Engineering – Center for Environmental Research and Technology (CE-CERT) in Riverside, CA, between July 2017 and May 2018. Chapter two will focus on observations obtained by utilizing the 37.5 m³ environmental chamber to evaluate the evolution of meat charbroiling emissions over time under atmospheric conditions. First, the results from these tests are compared to other published results for primary meat charbroiling emissions, then the aging and the changing character of these emissions are discussed. Last, the secondary impact from this emission source is evaluated and the percent SOA produced is calculated. Chapter three will focus on observations obtained by conducting experiments with the APL's new 14 L oxidation flow reactor (OFR) to evaluate meat charbroiling emissions. The mass spectra obtained by these experiments are compared to the spectra obtained from the

environmental chamber experiments. The aging of these emissions is again discussed, and the further change in character of these emissions is addressed. The results obtained from the OFR are then combined with the environmental chamber results to develop a more comprehensive understanding of the secondary impact of this source and percent SOA is calculated using a linear combination of variables. Chapter four will summarize the work presented in this thesis.

References

- AQMD, 2016. Final 2016 Air Quality Management Plan.
<http://www.aqmd.gov/docs/default-source/clean-air-plans/air-quality-management-plans/2016-air-quality-management-plan/final-2016-aqmp/final2016aqmp.pdf?sfvrsn=15> (2016)
- Araujo, J. A., & Nel, A. E. (2009). Particulate matter and atherosclerosis: role of particle size, composition and oxidative stress. *Particle and fibre toxicology*, 6(1), 24.
- BéruBé, K., Balharry, D., Sexton, K., Koshy, L., & Jones, T. (2007). Combustion-derived nanoparticles: Mechanisms of pulmonary toxicity. *Clinical and Experimental Pharmacology and Physiology*, 34(10), 1044-1050.
- Breyse, P. N., Delfino, R. J., Dominici, F., Elder, A. C., Frampton, M. W., Froines, J. R., ... & Koutrakis, P. (2013). US EPA particulate matter research centers: summary of research results for 2005–2011. *Air Quality, Atmosphere & Health*, 6(2), 333-355.
- Cheng, S., Wang, G., Lang, J., Wen, W., Wang, X., & Yao, S. (2016). Characterization of volatile organic compounds from different cooking emissions. *Atmospheric Environment*, 145, 299-307.
- Derwent, R. G., & Jenkin, M. E. (1991). Hydrocarbons and the long-range transport of ozone and PAN across Europe. *Atmospheric Environment. Part A. General Topics*, 25(8), 1661-1678.
- Derwent, R. G., Jenkin, M. E., & Saunders, S. M. (1996). Photochemical ozone creation potentials for a large number of reactive hydrocarbons under European conditions. *Atmospheric Environment*, 30(2), 181-199.
- Derwent, R. G., Jenkin, M. E., Saunders, S. M., & Pilling, M. J. (1998). Photochemical ozone creation potentials for organic compounds in northwest Europe calculated with a master chemical mechanism. *Atmospheric environment*, 32(14-15), 2429-2441.
- Donahue, N. M., Robinson, A. L., Stanier, C. O., & Pandis, S. N. (2006). Coupled partitioning, dilution, and chemical aging of semivolatile organics. *Environmental Science & Technology*, 40(8), 2635-2643.
- Gysel, N., Welch, W. A., Chen, C. L., Dixit, P., Cocker, D. R., & Karavalakis, G. (2017). Particulate matter emissions and gaseous air toxic pollutants from commercial meat cooking operations. *Journal of Environmental Sciences*.

- Hayes, P. L., Carlton, A. G., Baker, K. R., Ahmadov, R., Washenfelder, R. A., Alvarez, S., ... & Zotter, P. (2015). Modeling the formation and aging of secondary organic aerosols in Los Angeles during CalNex 2010. *Atmospheric chemistry and physics*, 15(10), 5773-5801.
- Hildemann, L. M., Klinedinst, D. B., Klouda, G. A., Currie, L. A., & Cass, G. R. (1994). Sources of urban contemporary carbon aerosol. *Environmental science & technology*, 28(9), 1565-1576.
- IARC, 2006. Overall Evaluation of Carcinogenicity to Human, Formaldehyde [50-00-0]. Monograph Series International Agency for Research on Cancer, Lyon, France.
- Jimenez, J. L., Canagaratna, M. R., Donahue, N. M., Prevot, A. S. H., Zhang, Q., Kroll, J. H., ... & Aiken, A. C. (2009). Evolution of organic aerosols in the atmosphere. *Science*, 326(5959), 1525-1529.
- Kelly, F. J., & Fussell, J. C. (2011). Air pollution and airway disease. *Clinical & Experimental Allergy*, 41(8), 1059-1071.
- Klein, F., Platt, S. M., Farren, N. J., Detournay, A., Bruns, E. A., Bozzetti, C., ... & Slowik, J. G. (2016). Characterization of gas-phase organics using proton transfer reaction time-of-flight mass spectrometry: Cooking emissions. *Environmental science & technology*, 50(3), 1243-1250.
- Kreyling, W. G., Semmler-Behnke, M., & Möller, W. (2006). Health implications of nanoparticles. *Journal of Nanoparticle Research*, 8(5), 543-562.
- Li, N., Bhattacharya, P., Karavalakis, G., Williams, K., Gysel, N., & Rivera-Rios, N. (2014). Emissions from commercial-grade charbroiling meat operations induce oxidative stress and inflammatory responses in human bronchial epithelial cells. *Toxicology reports*, 1, 802-811.
- Li, S., Williams, G., Jalaludin, B., & Baker, P. (2012). Panel studies of air pollution on children's lung function and respiratory symptoms: a literature review. *Journal of Asthma*, 49(9), 895-910.
- McDonald, J. D., Zielinska, B., Fujita, E. M., Sagebiel, J. C., Chow, J. C., & Watson, J. G. (2003). Emissions from charbroiling and grilling of chicken and beef. *Journal of the Air & Waste Management Association*, 53(2), 185-194.
- Mohr, C., Huffman, J. A., Cubison, M. J., Aiken, A. C., Docherty, K. S., Kimmel, J. R., ... & Jimenez, J. L. (2009). Characterization of primary organic aerosol emissions from meat cooking, trash burning, and motor vehicles with high-resolution aerosol mass spectrometry and comparison with ambient and chamber observations. *Environmental science & technology*, 43(7), 2443-2449.

- Oberdörster, G., Oberdörster, E., & Oberdörster, J. (2005). Nanotoxicology: an emerging discipline evolving from studies of ultrafine particles. *Environmental health perspectives*, 113(7), 823.
- Pelucchi, C., Negri, E., Gallus, S., Boffetta, P., Tramacere, I., & La Vecchia, C. (2009). Long-term particulate matter exposure and mortality: a review of European epidemiological studies. *BMC public health*, 9(1), 453.
- Roe, S. M., Spivey, M. D., Lindquist, H. C., Hemmer, P., & Huntley, R. (2004, June). National emissions inventory for commercial cooking. In 13th International Emission Inventory Conference, Clearwater, FL.
- Rogge, W. F., Hildemann, L. M., Mazurek, M. A., Cass, G. R., & Simoneit, B. R. (1991). Sources of fine organic aerosol. 1. Charbroilers and meat cooking operations. *Environmental Science & Technology*, 25(6), 1112-1125.
- Rumchev, K., Spickett, J., Bulsara, M., Phillips, M., & Stick, S. (2004). Association of domestic exposure to volatile organic compounds with asthma in young children. *Thorax*, 59(9), 746-751.
- Schauer, J. J., Kleeman, M. J., Cass, G. R., & Simoneit, B. R. (1999). Measurement of emissions from air pollution sources. 1. C1 through C29 organic compounds from meat charbroiling. *Environmental Science & Technology*, 33(10), 1566-1577.
- Shah, A. S., Langrish, J. P., Nair, H., McAllister, D. A., Hunter, A. L., Donaldson, K., ... & Mills, N. L. (2013). Global association of air pollution and heart failure: a systematic review and meta-analysis. *The Lancet*, 382(9897), 1039-1048.
- Utell, M. J., & Frampton, M. W. (2000). Acute health effects of ambient air pollution: the ultrafine particle hypothesis. *Journal of aerosol medicine*, 13(4), 355-359.
- Wang, Hongli & Xiang, Zhiyuan & Wang, Lina & Jing, Shengao & Lou, Shengrong & Tao, Shikang & Liu, Jing & Yu, Mingzhou & Li, Li & Lin, Li & Chen, Ying & Wiedensohler, Alfred & Chen, Changhong. (2017). Emissions of volatile organic compounds (VOCs) from cooking and their speciation: A case study for Shanghai with implications for China. *Science of the Total Environment*. 621. 10.1016/j.scitotenv.2017.10.098.
- Zhao, Y., Hu, M., Slanina, S., & Zhang, Y. (2007). The molecular distribution of fine particulate organic matter emitted from Western-style fast food cooking. *Atmospheric Environment*, 41(37), 8163-8171.

Chapter 2

Environmental Chamber Evaluation of Meat Charbroiling Emissions

2.1 Introduction

Environmental chambers are typically used to study photochemical air pollution under realistic conditions with the purpose of evaluating gas-phase and secondary aerosol mechanisms. This method of research allows for more control over what is studied with more comprehensive measurements than is typically achieved with ambient observations. Environmental chambers have been utilized for decades to help develop a better understanding of how specific compounds behave and change under atmospheric conditions (Carter *et al.*, 2004; Cocker *et al.*, 2001). More recently, environmental chambers have been used to evaluate how emissions sampled directly from the source of interest react under atmospheric conditions. Frequent subjects of such tests include diesel exhaust, exhaust from specific models of cars, or exhaust from wood smoke (e.g. Grieshop *et al.*, 2009; Nakao *et al.*, 2011; Weitkamp *et al.*, 2007). Such studies have been invaluable in furthering our understanding of the behavior of these emissions, their atmospheric impact, and often assist in creating new regulations. Thus, a natural next step in this line of research would be to use this powerful research tool to inspect a growing source of pollution for the Southern California Air Basin: commercial cooking emissions.

As previously stated, commercial cooking operations have become the single greatest primary source of fine particulate matter (PM_{2.5}) in the Southern California Air Basin (AQMD, 2016). Furthermore, it has been established that these emissions originate primarily from the charbroiling of fatty meats (Hildemann *et al.*, 1994; McDonald *et al.*,

2003; Mohr *et al.*, 2003). Thus, for the research presented here, a conventional backyard barbeque grill was used to charbroil hamburgers and generate emissions representative of the commercial cooking emissions of interest. A sampling line was set up to capture a portion of the exhaust, dilute the emissions, and transfer them to the 37.5 m³ environmental chamber located inside the Atmospheric Process Laboratory (APL) at the College of Engineering – Center for Environmental Research and Technology (CE-CERT) in Riverside, CA. Once the emissions were collected and diluted inside of the chamber, hydrogen peroxide was injected as a source of hydroxyl radicals and the chamber was exposed to ultraviolet (UV) radiation via multiple black lights as a representative source of sunlight. Together, these variables help to simulate atmospheric conditions in a controlled manner. Additionally, a series of experiments were conducted using a Teflon filter to remove the primary particulate matter (PM) emissions prior to injection into the chamber. These filtered tests were designed to study the gas-only emissions from meat charbroiling.

Much work has been done to document the quantity and type of primary emissions from meat charbroiling, but little research has been conducted regarding the evolution of these emissions in an environmental chamber under atmospheric conditions. The aim of this series of experiments is to evaluate how meat charbroiling emissions change over time, how these emissions oxidize under atmospheric conditions, and to estimate how much secondary organic aerosol (SOA) is formed from these primary PM and gas-phase emissions.

2.2 Experimental Methods

2.2.1 Sampling Methodology

For these experiments, a Char-Broil Classic 280 2-Burner Propane Gas Grill was situated outside of the laboratory and used to charbroil beef hamburger patties. The two propane burners were protected by flame guards and located 10 cm from the cooking grate. Hamburgers were cooked at medium setting and the charbroiler's cooking temperature ranged between 260 and 288° C. The meat used for these tests were Kirkland Signature ¼ lb. Ground Beef Hamburger Patties and contained 22% fat as stated by the manufacturer. The hamburger patties were cooked for four minutes on each side before being removed from the grilling surface and replaced with another frozen hamburger patty. Multiple hamburger patties were cooked at once to help reduce the variability of the emissions being sampled, since the concentration of emissions often spiked when hamburger patties were flipped. In this way, seven hamburger patties were cooked for approximately 30 minutes to generate the emission sample for each experiment.

The sampling line was designed to sample from the rear of the grill near the exhaust vents where the visible plume could be seen exiting the grill. The sample passed through an orifice and an ejector diluter within the first 30 cm of sample line. After two meters, the sample passed through a vented manifold and a second ejector diluter before being diluted a third and final time at a Y-joint before entering the environmental chamber. The environmental chamber was partially pre-filled with clean dilution air before sample injection so that the chamber would be completely full after sample injection. The compressed dilution air was set at 30 psi at the two ejector diluters and

approximately 37 psi min^{-1} at the Y-joint. Copper lines were used for the injection line and the total length of the injection line from sample intake outside to the upstairs environmental chamber was 21 meters. When desired, a Teflon filter (Pall PTFE $2.0 \mu\text{m}$ 47 mm) was added to the sampling line after all ejector diluters to filter out the primary PM from the emission sample. See Figure 2.1 for the schematic of this dilution sampling set-up.

Once the emission sample was collected and injected into the 37.5 m^3 environmental chamber, $84 \mu\text{L}$ of hydrogen peroxide was vaporized in a heating unit and injected into the environmental chamber. When exposed to UV radiation, this concentration of H_2O_2 is estimated to produce a concentration of hydroxyl radicals resembling that found under atmospheric conditions. Once all reactants were added to the chamber, the chamber's black lights were turned on and the experiment was permitted to

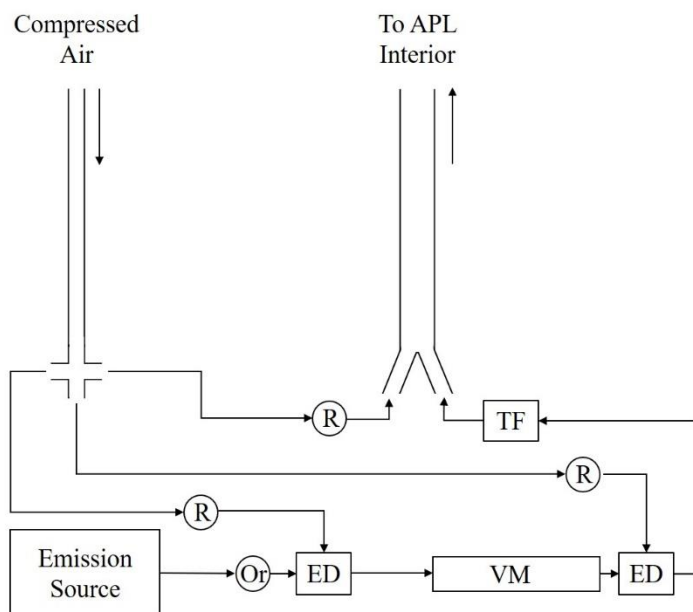


Figure 2.1. Schematic of dilution sample line set-up for chamber cooking experiments. Key: R – Rotameter, ED – ejector diluter, VM – vented manifold, Or – orifice, TF – Teflon filter, optional.

run for a minimum of four hours. Samples were continuously taken from the environmental chamber throughout the duration of the experiment for analysis. Three experiments were conducted each for unfiltered and filtered emissions with only the addition of hydrogen peroxide and UV radiation as reactants.

2.2.2 Instrumental Analysis

A High-Resolution Time of Flight Aerosol Mass Spectrometer (HR-ToF-AMS) manufactured by Aerodyne Research Inc. was used to characterize the primary organic aerosol (POA) as it was deposited into the chamber and the secondary organic aerosol (SOA) that was formed over the course of the experiment. The voltage of the Tungsten filament was 70eV and the vaporizer temperature was set at 600° C. The Scanning Mobility Particle Sizer (SMPS) used for these experiments was designed and assembled by the Cocker Lab Group. As with all SMPS instruments, this SMPS sizes particles based on the particle's electric mobility and operates on the assumption that the particles being analyzed are spherical. A Kanomax Aerosol Particle Mass (APM) analyzer, assembled by the Cocker Lab Group, was used to estimate the density of the aerosol being sampled and produced in conjunction with the SMPS. Last, a Volatility Tandem Differential Mobility Analyzer (VTDMA) was used to estimate the volatility of the aerosol being sampled and produced in the environmental chamber. The VTDMA used for these experiments was designed and assembled by the Cocker Lab Group.

2.2.3 Data Analysis

Data from the Aerodyne AMS was analyzed using Igor Pro 6.3.7.2 by Wavemetrics using the macros SQUIRREL v1.56D and PIKA v1.15D developed by the Jimenez Group at the University of Colorado, Boulder. A series of Microsoft Excel macros created by the Cocker Lab Group were used to analyze the data obtained from the SMPS and combine this information with data obtained by the APM and VTDMA. These macros were used to document experimental condition and raw data as well as calculate particle mass and volume over the course of the experiment. Two MATLAB functions created by the Cocker Lab Group were used to analyze data from the APM to calculate aerosol particle density and to analyze data obtained from the VTDMA to calculate the volume fraction remaining (VFR) respectively.

Angle theta (θ) was used throughout this research to quantify the change between mass spectra obtained by the AMS (Kostenidou *et al.*, 2009). Typically, angle theta is used when spectra are nearly identical since this method is much more precise than the Pearson correlation coefficient (Pearson's r) or the coefficient of determination (R^2). Mass spectra are written as vectors for this method of analysis then compared, with $\theta = 0$ for identical spectra and $\theta = 90$ degrees for completely opposing spectra.

2.3 Results and Discussion

2.3.1 Evaluating the Primary Organic Aerosol Emissions

Figure 2.2 shows a representative mass spectrum from the beginning of an unfiltered chamber run which corresponds with the primary organic aerosol (POA)

emissions from charbroiling hamburgers. The markers used in this figure and in future mass spectra, m/z 29, 41, 43, 55, 57 and 69, were chosen because they have been used as tracers for cooking-related organic aerosol (COA) in previous literature (He *et al.*, 2010; Mohr *et al.*, 2009, 2012). These prominent m/z fragments are associated with ions produced from saturated alkanes and alkenes, cycloalkanes, and oxygenated species like organic acids. Additionally, the excess of values above the m/z 44 fragment suggests that the molecules that compose this emission source have a large alkyl backbone with limited oxygen (Mohr *et al.*, 2009). This conclusion is supported by gas chromatography-mass spectroscopy (GC-MS) research conducted by Rogge *et al.* (1991) and Schauer *et al.* (1999).

Angle theta was utilized to compare the spectra in Figure 2.2 to the relevant spectra listed in the AMS Spectral Database (Ulbrich, Ulbrich *et al.*, 2009). Specifically, the spectrum for charbroiled fatty hamburger emissions provided by Mohr *et al.* (2009) was used for this assessment. To make a valid comparison to this spectrum, which evaluates the POA emissions from this source, a normalized average mass spectrum was created using a small sample of scans from the beginning of each unfiltered environmental chamber experiment to represent the primary emissions for the present work. The average angle theta value for the comparison between these two spectra was found to be 24.8 ± 0.4 degrees, which correlates to an R^2 value between 0.7 and 0.8. This illustrates that the spectra obtained for these experiments deviate appreciably from what has been previously considered a reference spectrum for primary fatty hamburger emissions, with the prevalent m/z 55 fragment being the only significant similarity. In

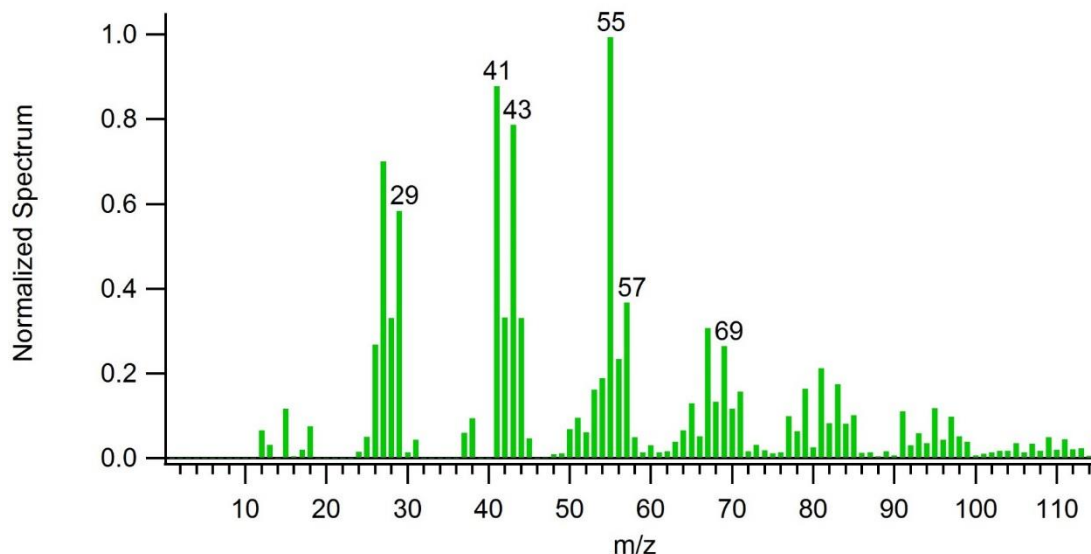


Figure 2.2. Normalized average mass spectrum obtained from initial measurements of an unfiltered environmental chamber experiment to represent primary organic aerosol (POA) created by charbroiling hamburgers. This spectrum is representative of the POA emissions seen for all three repeated unfiltered environmental chamber experiments.

contrast, the prominent m/z 27, 41, and 67 peaks provide the most readily visible differences between the spectra obtained by these experiments and Mohr *et al.* (2009)'s reference spectrum for this emission source.

2.3.2 Mechanism of Emission Aging

This section evaluates the aging of charbroiled hamburger emissions over time by comparing the results of the unfiltered and filtered environmental chamber experiments over the duration of at least four hours. Studying the aging of these emissions can yield valuable information about the potential reaction mechanism between the emissions of interest and common environmental reactants like hydroxyl radicals and ultraviolet radiation. Furthermore, establishing that these emissions are aging in the atmosphere

underscores the need to consider the secondary impact of these emissions, as emissions that age are considered to be participating in atmospheric chemical processes.

Triangle plots are often used for a quick visualization of how oxidized or aged a given set of emissions are. The y-axis on these plots is the ratio of m/z 44 to the total signal in the component spectrum (f_{44}) while the x-axis is the ratio of m/z 43 to the total signal in the component spectrum (f_{43}) (Ng *et al.*, 2011). The m/z 44 fragment is mostly composed of CO_2^+ under typical conditions and the m/z 43 fragment is composed mainly of $\text{C}_2\text{H}_3\text{O}^+$ or C_3H_7^+ depending on whether the emissions are oxidized or hydrocarbon-like. Generally, results from environmental chamber studies are found in the lower half of the triangle plot. This area is associated with semi-volatile oxidized organic aerosol (SVOOA) while the upper half of the triangle plot is associated with low-volatile oxidized organic aerosol (LVOOA) (Ng *et al.*, 2011). As emissions become more oxidized, they tend to travel towards the apex of the triangle plot, which represents the hypothetical ultimate oxidized state of atmospheric organic aerosol. Traditionally, ambient measurements tend to be found towards the top half of the triangle plot in this LVOOA area.

Figure 2.3 shows representative triangle plots for the unfiltered and filtered environmental chamber experiments. A clear trend can be seen in the unfiltered environmental chamber experiments as the emissions in the chamber became more oxidized over the duration of the experiment. Since the primary particulate emissions were allowed into the chamber, along with the gaseous emissions created by charbroiling meat, figure 2.3 a) is representative of the aging of the primary emissions from this

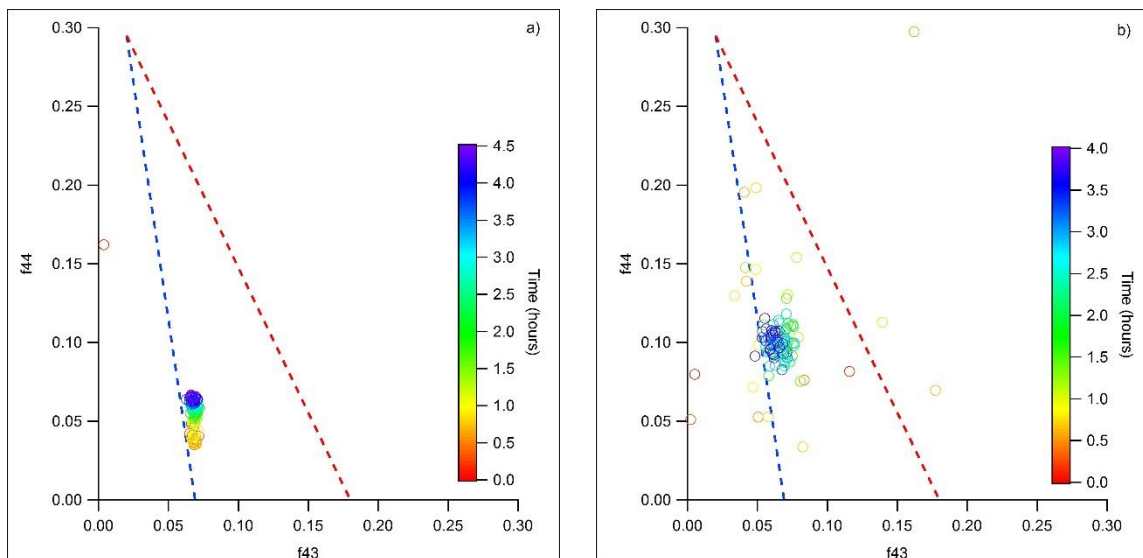


Figure 2.3. Representative triangle plots for a) unfiltered environmental chamber experiments and b) filtered environmental chamber experiments. A clear oxidative trend can be seen in the unfiltered experiments, representing the aging of primary particulate and gaseous emissions from charbroiling meat. This oxidative trend continues into the filtered environmental chamber experiments that represent only the SOA formation from the gaseous emissions generated by charbroiling meat. Greater scatter is seen in figure 2.3 b) due to the lower concentration of sample emissions present in the filtered experiments.

source. In other words, figure 2.3 a) illustrates the aging of both the POA and SOA created by this source. This oxidative trend continues in the filtered chamber experiments, as can be seen in figure 2.3 b), although greater scatter is seen in this figure due to the lower starting concentration of the gases present in the filtered environmental chamber experiments. Nonetheless, the gas-only emissions that were allowed into the chamber clearly created SOA, and this secondary aerosol was more oxidized than the aerosol formed in the previous unfiltered environmental chamber experiments.

Van Krevelen diagrams are also frequently used to ascertain oxidation information about emissions as they age. These diagrams have been around since 1950 (Van Krevelen, 1950), however, only recently have they been applied to atmospheric chemical processes (Heald *et al.*, 2010). These diagrams compare the emission's

hydrogen to carbon (H:C) ratios on the y-axis and the emission's oxygen to carbon (O:C) ratios on the x-axis. Information regarding the addition of functional groups via aging can be determined by the slope of the trend line through the AMS data plotted on this graph.

Figure 2.4 shows the representative Van Krevelen diagrams obtained from the unfiltered environmental chamber experiments and the filtered environmental chamber experiments. Due to the low starting concentration of gaseous emissions in the filtered experiments, the Van Krevelen diagrams for these experiments are noisy and potentially inconclusive. The emissions in both figure 2.4 a) and b) trend towards the right, with the filtered experiments showing an even greater O:C ratio than the unfiltered experiments. Increasing O:C ratios typically indicates atmospheric aging (DeCarlo *et al.*, 2008). Furthermore, for the unfiltered chamber experiments, the trend line has a slope of nearly

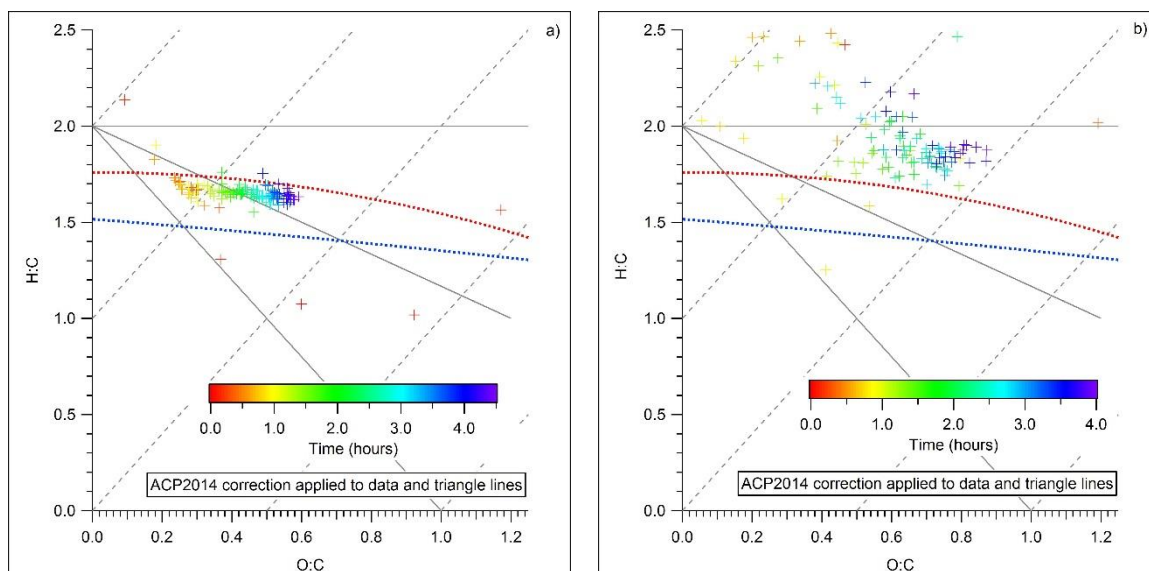


Figure 2.4. Representative Van Krevelen diagrams for a) unfiltered environmental chamber experiments and b) filtered environmental chamber experiments. Again, a trend of oxidation can be seen in the unfiltered chamber experiment that carries over to the filtered experiments, which show an increased oxidation from the unfiltered experiments. Due to the low concentrations of emissions in the filtered experiments, further conclusions from the Van Krevelen diagram shown in b) are inconclusive. From the slope in a), however, it can be hypothesized that alcohol and/or peroxide groups are being added to the meat charbroiling emissions as a mechanism of oxidation.

zero, indicating that oxygen atoms are being added to the emission's molecules while losing little to no hydrogen atoms in this process. This suggests that the oxidation pathway for these emissions involve the addition of alcohol and/or peroxide groups. These results differ from typical ambient measurements, which tend to have a slope of negative one and are generally hypothesized to have an oxidation pathway involving the addition of carboxylic acid (Heald *et al.*, 2010).

2.3.3 Character Change of Aging Emissions

A change in emission character was observed in the mass spectra obtained over the course of these experiments. Figure 2.5 shows four normalized spectra to illustrate this point. The spectra in figure 2.5 a) and b) are representative averages of the first five runs at the beginning of an unfiltered experiment and the last five runs from the end of the same unfiltered experiment, respectively. Likewise, the spectra shown in figure 2.5 c) and d) are representative averages of the first five runs at the beginning of a filtered experiment and the last five runs from the same filtered experiment. According to the hypothesis developed during testing, figure 2.5 a) is representative of the POA created by meat charbroiling while figure 2.5 b) is representative of POA created by the meat charbroiling itself plus the SOA created during the aging of those primary emissions. Meanwhile, figure 2.5 c) is representative of the SOA created solely from the gas phase emissions generated by meat charbroiling and figure 2.5 d) represents the aging of this SOA derived from these gaseous emissions. Appreciable changes can be seen from the start of each individual experiment to the end of the same experiment, but a deeper

understanding of the diverse character of meat charbroiling emissions that can be found in the ambient atmosphere can be gained when comparing figures 2.5 a) and d).

From the beginning of the unfiltered experiments to the end of the unfiltered experiments, figure 2.5 a) to b), there is an average change in angle theta of 19.3 ± 2.6 degrees. The two spectra are noticeably different at this point and correspond to an R^2 value between 0.7 and 0.8. Key peak changes are the increase of m/z 28, 29, 43, 44, and 57 and corresponding decrease of m/z 41, 55, 67. A couple of the prominent peaks have remained relatively stationary as well, such as m/z 27 and 69. However, many of these peaks are associated with both a hydrocarbon molecule and their oxidized equivalent, so these observations alone do not yield enough information without examining the high-resolution (HR) data. The HR data was examined in detail for three peaks in particular:

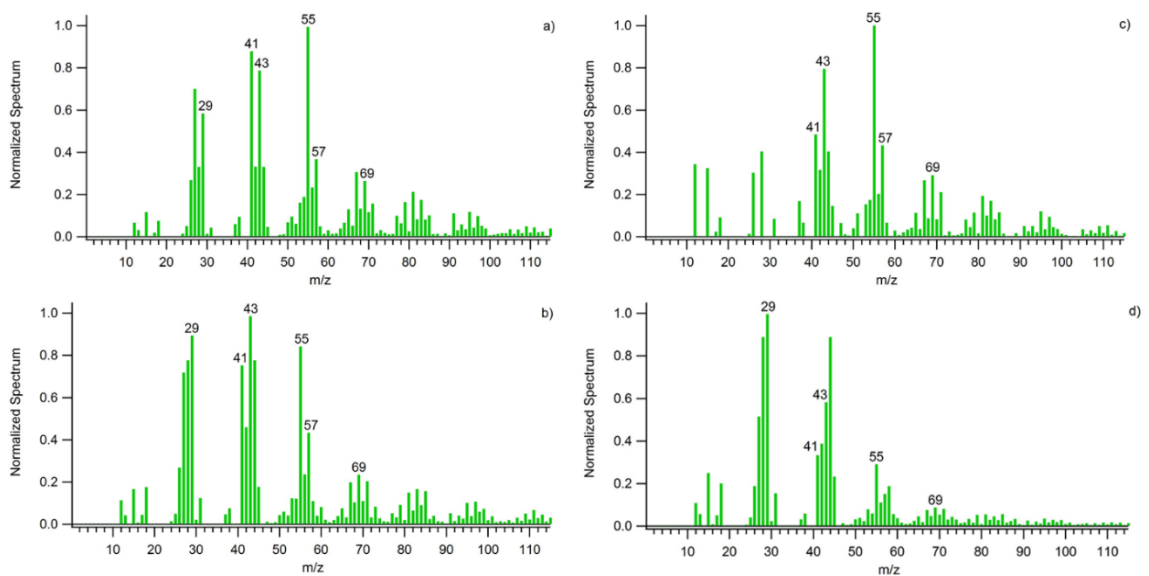


Figure 2.5. Representative normalized mass spectra for the average of the a) first five runs at the beginning of an unfiltered experiment, b) last five runs at the end of an unfiltered experiment, c) first five runs at the beginning of a filtered experiment, and d) last five runs at the end of a filtered experiment. Theoretically, a) represents the fresh POA generated by meat charbroiling, b) represents the aged POA and SOA generated by meat charbroiling, c) represents the SOA formed by the primary gas-only emissions of meat charbroiling, and d) represents the aged SOA formed from the gas-only emissions of meat charbroiling.

m/z 29, 43, and 55. This data, displayed in table 2.1, shows a shift from a roughly 50:50 composition of the hydrocarbon ion to oxidized ion at the beginning of these experiments to a ratio that clearly favors the oxidized ion by the end of the experiment for each fragment analyzed.

Comparing the beginning of the filtered experiments to the end of the filtered experiments, figures 2.5 c) and d) respectively, yield a far more drastic change between the beginning and ending spectra. The angle theta for this comparison is 51.8 ± 3.5 degrees, correlating to an R^2 value of less than 0.7. The significant change between the start and finish of the filtered experiments likely results from a different, far more reactive kind of aerosol being formed from the gas-only emissions than the aerosol that develops alongside the primary PM emissions. The most noticeable changes in spectra from the start of these experiments to the end of these experiments is the sharp increase in m/z 27, 28, 29, and 44 while m/z 43, 55, 57, and 69 show a sharp decrease. With the

Experiment Type	m/z 29: CHO ⁺ /C ₂ H ₅ ⁺	m/z 43: C ₂ H ₃ O ⁺ /C ₃ H ₇ ⁺	m/z 55: C ₃ H ₃ O ⁺ /C ₄ H ₇ ⁺
Unfiltered at Start, Environmental (POA)	1.01	0.79	0.93
Unfiltered at End, Environmental (POA and SOA)	2.36	1.38	1.10
Filtered Average, Environmental (SOA)	19.8	3.68	1.22

Table 2.1. Table illustrating how the composition of meat charbroiling emissions for a sample of prominent fragments from these experiments became more oxidized over time. The numbers presented here are an average of three sets of data each for the start of the unfiltered experiments (POA), the end of the unfiltered experiments (POA and SOA), and the end of the filtered experiments (SOA). These values emphasize the importance of evaluating the high-resolution data along with the mass spectra for cooking emission experiments.

sudden dominance of the m/z 29 and 44 peaks, CHO^+ and CO_2^+ respectively, these findings help support the hypothesis that the meat charbroiling emissions are initially composed of molecules with long-chain alkyl backbones containing limited oxygen that degrade via atmospheric aging into smaller and more common molecules.

Figure 2.6 shows representative mass spectra from the beginning and end of unfiltered and filtered environmental chamber experiments evaluating meat charbroiling emissions. These spectra show the full signature of the aerosol evaluated by the AMS during testing, including NO_3 , SO_4 , NH_4 , and Cl ions. From figure 2.6 a) to b), respectively representing the start and finish of unfiltered experiments, an increase in NO_3 containing compounds is seen. This increase in NO_3 signature seems to continue in the filtered experiments, as seen in figure 2.6 c) and d). However, this increase may appear artificially important due to the low starting concentration of the starting sample

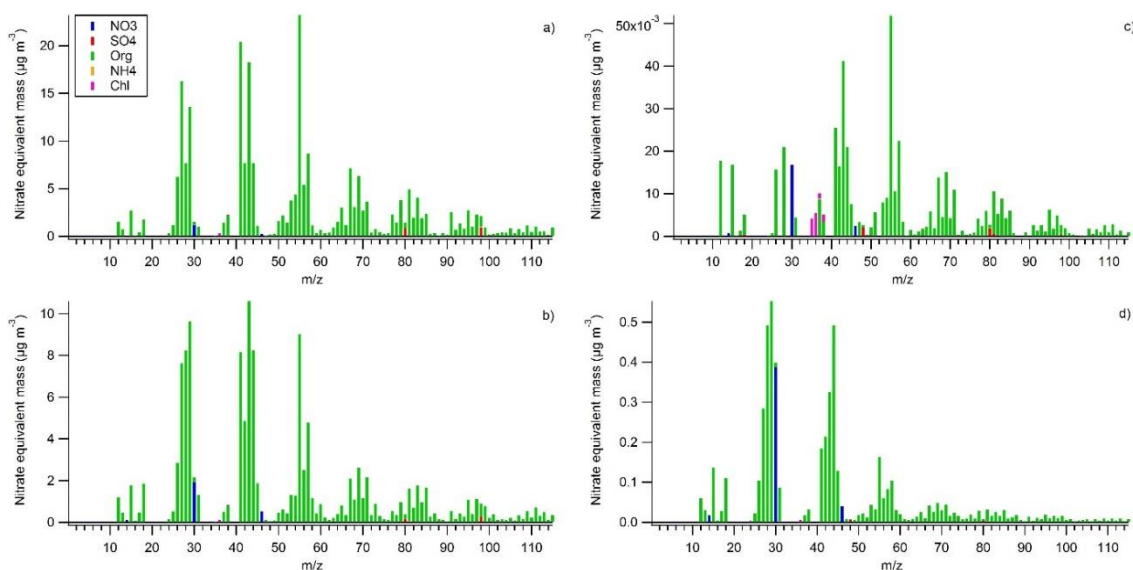


Figure 2.6. Representative average mass spectra of meat charbroiling emissions taken from a) the beginning of an unfiltered experiment, b) the end of an unfiltered experiment, c) the beginning of a filtered experiment, and d) the end of a filtered experiment. In both experiments, an increase in NO_3 compounds and a decrease in SO_4 compounds can be observed.

in the filtered environmental chamber experiments. Overall, SO₄ containing ions appear to decrease from beginning to end of experiments. A relatively large Cl trace is seen in figure 4.6 c) at the start of the filtered experiments, but nearly disappears by the end.

2.3.4 Percent Secondary Organic Aerosol Production

The following equation, originally used by Chirico *et al.* (2010), was applied to the current research to calculate the percent secondary organic aerosol (%SOA) produced at time t by charbroiled meat emissions:

$$\%SOA(t) = [OM(t) - \left(\frac{C_4H_9^+(t)}{C_4H_9^+(t_0)}\right)OM(t_0)] \times 100, \quad (2.1)$$

where

$OM(t)$ is the total organic matter at time t ,

$OM(t_0)$ is the total organic matter before exposure to UV radiation,

$C_4H_9^+(t)$ is the non-oxygenated portion of m/z 57 at time t , and

$C_4H_9^+(t_0)$ is the non-oxygenated portion of m/z 57 before exposure to UV radiation.

The fragment m/z 57 was chosen for this calculation due to its predominate association with primary species. In the original research regarding diesel exhaust, the m/z 57 fragment was also used because C₄H₉⁺ is a dominate ion in aerosols generated by diesel engines. The m/z 57 fragment was also used for the SOA analysis presented here since it was a notable fragment in the charbroiled meat emissions as well. High resolution results from the AMS data was utilized to separate the C₄H₉⁺ portion from the oxygenated C₃H₃O⁺ portion of the m/z 57 fragment for use with the above equation.

The results of this analysis can be seen in figure 2.7. The percent primary organic aerosol (%POA) is shown on the left y-axis and the corresponding %SOA is shown on the right y-axis. The data is plotted versus time on the x-axis over the course of the experiment after the black lights have been turned on. The unfiltered experiments, which were expected to represent how the POA and SOA created by meat charbroiling changed over time, showed the greatest change from start to finish. On average, the unfiltered experiments contained of $13 \pm 5.6\%$ SOA at one hour and $24 \pm 6.7\%$ by the end of the

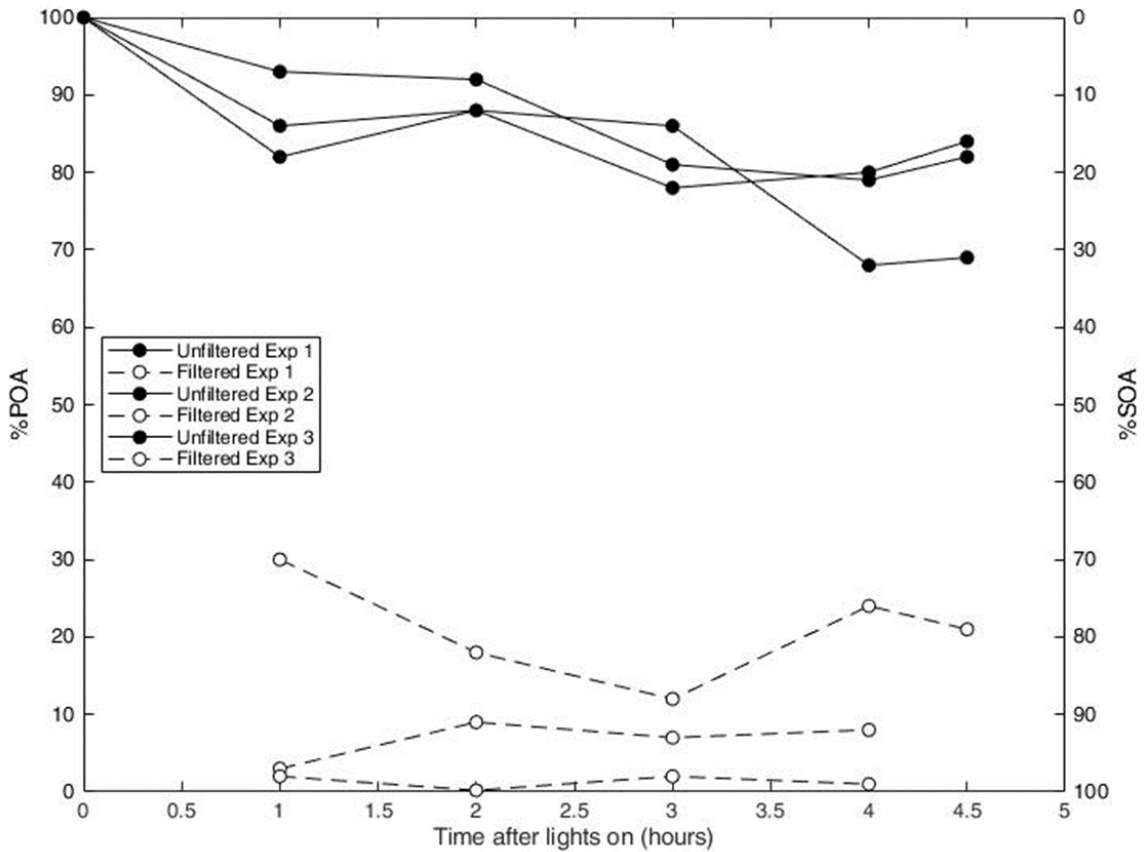


Figure 2.7. Graphical illustration of percent primary organic aerosol (%POA) and percent secondary organic aerosol (%SOA) versus time over the course of an environmental chamber experiment after the black lights have been turned on. Unfiltered experiments are shown with solid lines and black dots while filtered experiments are shown with dashed lines and white dots. The unfiltered experiments showed the greatest change over time, on average changing from $13 \pm 5.6\%$ SOA at one hour to $24 \pm 6.7\%$ SOA after four hours. The filtered experiments showed less change from start to finish, however, and instead contained $90 \pm 9.8\%$ SOA on average.

experiment after four hours with the black lights on. With the current data, it is unclear if this trend would have continued to generate more SOA or if the SOA production was beginning to plateau at this point. The filtered experiments, which were expected to represent purely SOA created by the gaseous emissions of meat charbroiling, did not show a significant change from start to finish in this series of experiments. On average, the emissions from the filtered experiments consisted of $90 \pm 9.8\%$ SOA. This suggests that there may be a consistent average SOA production rate produced by the gaseous emissions of meat charbroiling.

2.4 Summary

The unfiltered and filtered emissions from the charbroiling of beef hamburger patties were studied under typical atmospheric conditions using a 37.5 m^3 environmental chamber at CE-CERT. The aim of this set of experiments was to evaluate how the meat charbroiling emissions changed over time under atmospheric conditions, with the unfiltered experiments representing the aging of both the POA and SOA created by this source and filtered experiments representing the aging of only the SOA created by this source. The initial AMS spectra of the emissions, taken at the beginning of unfiltered experiments before exposure to hydroxyl radicals and UV radiation, found spectra that deviated appreciably from spectra previously considered as a reference for primary hamburger emissions provided by Mohr *et al.* in 2009. The average angle theta for this comparison of primary emissions between the unfiltered initial spectra and the spectra used as a reference for fatty hamburger charbroiling was found to be 24.8 ± 0.4 degrees,

which corresponds to an R^2 value between 0.7 and 0.8. This deviation suggests that more research is needed to identify a standard, if it exists among the many variables, for hamburger charbroiling emissions.

The hamburger charbroiling emissions examined here were observed to age considerably over time in all experiments, with the unfiltered chamber experiments exhibiting greater aging over the course of the experiment and the unfiltered experiments exhibit a greater oxidation overall. The triangle plots and Van Krevelen diagrams for these experiments, figure 2.3 and 2.4 respectively, clearly illustrate this finding. Additionally, the slope obtained from the Van Krevelen diagram suggests that the oxidative pathway for the aging of these emissions involve the addition of alcohol and/or peroxide groups. This finding differs from typical ambient measurements, which tend to oxidize via the addition of carboxylic acid groups.

Since these emissions clearly oxidize under normal atmospheric conditions, it can be verified that emissions from meat charbroiling are chemically active and take part in atmospheric chemistry both as PM and as gases. This is supported by the AMS spectra taken from both experiment types over the duration of each experiment. Such sampling of spectra has revealed the changing character of meat charbroiling emissions over time, overall showing a significant shift towards smaller fragments in both experiment types. For the unfiltered experiments, the angle theta observed between the spectra from the beginning and the end of the experiment was on average 19.3 ± 2.6 degrees. This angle theta value correlates to an R^2 value between 0.7 and 0.8 and represents a significant difference in spectra. However, an even more pronounced change is observed between

the start and finish of filtered experiments with an angle theta of 51.8 ± 3.5 degrees and an associated R^2 value of less than 0.7. The significant change for the filtered experiments likely results from a different kind of aerosol being formed from the gas-only emissions as opposed to those that develop from the interactions between primary PM emissions and gaseous emissions found in the unfiltered experiments. Furthermore, this suggests that the aerosol formed from the gas-only emissions are far more reactive than those formed along with the primary PM emissions.

Further insights can be gleaned by inspecting the HR data from the AMS, as most of the peaks of interest are associated with both a hydrocarbon ion and an oxidized ion. The HR data was examined in detail for three peaks in particular: m/z 29, 43, and 55. The ratio between hydrocarbon ions and oxidized ions in the unfiltered experiments was nearly 50:50 in the unfiltered experiments and shifted to clearly favor the oxidized ions by the end of the filtered experiments. This illustrates the need to utilize the high-resolution data provided by the AMS to fully understand the meaning of changes observed in mass spectra for this emission source.

Last, the percent SOA created from the meat charbroiling emissions was calculated using a method originally described in paper published by Chirico *et al.* in 2010. On average, the unfiltered experiments consisted of $13 \pm 5.6\%$ SOA after one hour and $24 \pm 6.7\%$ after four hours with the black lights on. It is unclear whether the data plateaus at this point or whether it will continue to create more SOA if given more time to age. The filtered experiments remained more constant, averaging $90 \pm 9.8\%$ SOA throughout the experiment. These findings back up the earlier hypothesis that the

unfiltered experiments represent the evolution of both the POA and SOA generated by meat charbroiling while the filtered experiments represent the SOA generated by meat charbroiling. They also clearly communicate the importance of considering the secondary impact of emissions from meat charbroiling. The gaseous emissions especially have a dramatic potential to create significant amounts of secondary organic aerosol. However, with commercial cooking rising to the top contributor of fine particulate matter pollution in the South Coast Air Basin, the secondary impacts from both the POA and SOA emissions created by meat charbroiling clearly need to be considered with greater accuracy and understanding.

2.5 References

- AQMD, 2016. Final 2016 Air Quality Management Plan.
<http://www.aqmd.gov/docs/default-source/clean-air-plans/air-quality-management-plans/2016-air-quality-management-plan/final-2016-aqmp/final2016aqmp.pdf?sfvrsn=15> (2016)
- Carter, W. P., Cocker III, D. R., Fitz, D. R., Malkina, I. L., Bumiller, K., Sauer, C. G., ... & Song, C. (2005). A new environmental chamber for evaluation of gas-phase chemical mechanisms and secondary aerosol formation. *Atmospheric Environment*, 39(40), 7768-7788.
- Chirico, R., DeCarlo, P. F., Heringa, M. F., Tritscher, T., Richter, R., Prévôt, A. S. H., ... & Laborde, M. (2010). Impact of aftertreatment devices on primary emissions and secondary organic aerosol formation potential from in-use diesel vehicles: results from smog chamber experiments. *Atmospheric Chemistry & Physics Discussions*, 10(6).
- Cocker, D. R., Flagan, R. C., & Seinfeld, J. H. (2001). State-of-the-art chamber facility for studying atmospheric aerosol chemistry. *Environmental science & technology*, 35(12), 2594-2601.
- DeCarlo, P. F., Dunlea, E. J., Kimmel, J. R., Aiken, A. C., Sueper, D., Crouse, J., ... & Zhou, J. (2008). Fast airborne aerosol size and chemistry measurements above Mexico City and Central Mexico during the MILAGRO campaign. *Atmospheric Chemistry and Physics*, 8(14), 4027-4048.
- Grieshop, A. P., Logue, J. M., Donahue, N. M., & Robinson, A. L. (2009). Laboratory investigation of photochemical oxidation of organic aerosol from wood fires 1: measurement and simulation of organic aerosol evolution. *Atmospheric Chemistry and Physics*, 9(4), 1263-1277.
- He, L. Y., Lin, Y., Huang, X. F., Guo, S., Xue, L., Su, Q., ... & Zhang, Y. H. (2010). Characterization of high-resolution aerosol mass spectra of primary organic aerosol emissions from Chinese cooking and biomass burning. *Atmospheric Chemistry and Physics*, 10(23), 11535-11543.
- Heald, C. L., Kroll, J. H., Jimenez, J. L., Docherty, K. S., DeCarlo, P. F., Aiken, A. C., ... & Artaxo, P. (2010). A simplified description of the evolution of organic aerosol composition in the atmosphere. *Geophysical Research Letters*, 37(8).
- Hildemann, L. M., Klinedinst, D. B., Klouda, G. A., Currie, L. A., & Cass, G. R. (1994). Sources of urban contemporary carbon aerosol. *Environmental science & technology*, 28(9), 1565-1576.

- Kostenidou, E., Lee, B. H., Engelhart, G. J., Pierce, J. R., & Pandis, S. N. (2009). Mass spectra deconvolution of low, medium, and high volatility biogenic secondary organic aerosol. *Environmental science & technology*, 43(13), 4884-4889.
- Mohr, C., Huffman, J. A., Cubison, M. J., Aiken, A. C., Docherty, K. S., Kimmel, J. R., ... & Jimenez, J. L. (2009). Characterization of primary organic aerosol emissions from meat cooking, trash burning, and motor vehicles with high-resolution aerosol mass spectrometry and comparison with ambient and chamber observations. *Environmental science & technology*, 43(7), 2443-2449.
- Mohr, C., DeCarlo, P. F., Heringa, M. F., Chirico, R., Slowik, J. G., Richter, R., ... & Peñuelas, J. (2012). Identification and quantification of organic aerosol from cooking and other sources in Barcelona using aerosol mass spectrometer data. *Atmospheric Chemistry and Physics*, 12(4), 1649-1665.
- McDonald, J. D., Zielinska, B., Fujita, E. M., Sagebiel, J. C., Chow, J. C., & Watson, J. G. (2003). Emissions from charbroiling and grilling of chicken and beef. *Journal of the Air & Waste Management Association*, 53(2), 185-194.
- Nakao, S., Shrivastava, M., Nguyen, A., Jung, H., & Cocker III, D. (2011). Interpretation of secondary organic aerosol formation from diesel exhaust photooxidation in an environmental chamber. *Aerosol Science and Technology*, 45(8), 964-972.
- Ng, N. L., Canagaratna, M. R., Jimenez, J. L., Chhabra, P. S., Seinfeld, J. H., & Worsnop, D. R. (2011). Changes in organic aerosol composition with aging inferred from aerosol mass spectra. *Atmospheric Chemistry and Physics*, 11(13), 6465-6474.
- Rogge, W. F., Hildemann, L. M., Mazurek, M. A., Cass, G. R., & Simoneit, B. R. (1991). Sources of fine organic aerosol. 1. Charbroilers and meat cooking operations. *Environmental Science & Technology*, 25(6), 1112-1125.
- Schauer, J. J., Kleeman, M. J., Cass, G. R., & Simoneit, B. R. (1999). Measurement of emissions from air pollution sources. 1. C1 through C29 organic compounds from meat charbroiling. *Environmental Science & Technology*, 33(10), 1566-1577.
- Ulbrich, I. M., Canagaratna, M. R., Zhang, Q., Worsnop, D. R., & Jimenez, J. L. (2009). Interpretation of organic components from Positive Matrix Factorization of aerosol mass spectrometric data. *Atmospheric Chemistry and Physics*, 9(9), 2891-2918.
- Ulbrich, I.M., Handschy, A., Lechner, M., and Jimenez, J.L. AMS Spectral Database. URL: <http://cires.colorado.edu/jimenez-group/AMSSd/>

Van Krevelen, D. W. (1950). Graphical-statistical method for the study of structure and reaction processes of coal. *Fuel*, 29, 269-284.

Weitkamp, E. A., Sage, A. M., Pierce, J. R., Donahue, N. M., & Robinson, A. L. (2007). Organic aerosol formation from photochemical oxidation of diesel exhaust in a smog chamber. *Environmental science & technology*, 41(20), 6969-6975.

Chapter 3

Oxidation Flow Reactor Evaluation of Meat Charbroiling Emissions

3.1 Introduction

Potential aerosol mass (PAM) is a concept pioneered by Kang *et al.* in 2007 who defined the term as the maximum amount of aerosol that the oxidation of precursor emissions can produce. PAM chambers, also known as oxidation flow reactors (OFR), have since been developed that operate with extreme concentrations of oxidants to produce rapid oxidation to low volatility compounds, ultimately resulting in aerosol production (Kang *et al.*, 2007). The purpose of OFRs is to find the hypothetical maximum aerosol yield that a given initial chemical or emission source can produce. OFRs are designed as small flow-through photo-oxidation reactors with extremely high hydroxyl radical and ozone concentrations (Kang *et al.*, 2011). These flow-through chambers typically have a volume of 0.001 – 0.01 m³ that produce a residence time of seconds to minutes (Lambe *et al.*, 2011). The equivalent atmospheric exposure from these flow-through PAM chambers and OFRs generally represents several days to two weeks despite the small residence times involved (Kang *et al.*, 2011; Lambe *et al.*, 2011), assuming an average atmospheric hydroxyl radical concentration of 1.5×10^6 molecules cm⁻³ (Mao *et al.*, 2009). Mercury lamps are typically used as the ultraviolet radiation source in these chambers. Ozone can be produced externally using an ozone generator or internally as part of the chemistry with aerosolized water and ultraviolet radiation. Aerosolized water is produced externally with a bubbler and injected along with the

purified flow air. Extensive descriptions of PAM theory and typical schematics is described in detail elsewhere (Kang *et al.*, 2007, 2011; Lambe *et al.*, 2011, 2015).

OFRs have their advantages over traditional environmental chambers, though they have their own spectrum of concerns. OFRs are specifically designed to minimize surface-to-volume ratio in an effort to diminish wall effects. Wall loss, that is the change in particle number concentrations due to deposition on chamber walls, is a significant concern in traditional environmental chambers and requires correcting for during the post-processing of data obtained from these chambers (Cocker *et al.*, 2001). Recently, Lambe *et al.* (2011) established that vapor wall losses in OFRs are negligible and thus provides one clear advantage to using OFRs over environmental chambers. Additionally, OFRs show the potential to oxidize precursor emissions past what was previously obtainable in environmental chambers and thus resulting in aged emissions closer to that found under ambient conditions. Another apparent advantage to using OFRs over environmental chambers is the time it takes to run an experiment. Environmental chambers are not designed to track the fast changes of precursor gases in the atmosphere (Kang *et al.*, 2007), with experimental times measured in hours to days whereas an OFR can yield measurements in seconds to minutes. Likewise, OFRs are generally smaller in size and tend to be more portable than environmental chambers.

However, there is at least one major concern with the high hydroxyl radical concentrations required for the intense oxidation obtained by OFRs. Traditional environmental chambers, with their longer residence times and lower oxidant concentrations, may more accurately emulate atmospheric aging (Lambe *et al.*, 2011).

Specifically, many researchers have concerns over the high oxidant concentration causing underestimated SOA yields due to changing the chemistry by which the emissions are aging (Chacon-Madrid and Donahue, 2011; Kroll *et al.*, 2009; Lambe *et al.*, 2012). At least one study has compared results from an environmental chamber and an OFR (Bruns *et al.*, 2015), but much work is yet needed to suss out the nuances of each oxidation system. Matsunaga and Ziemann (2010) pointed out that all laboratory reactors are imperfect simulations of the atmosphere due to walls that cause particle loss and potentially influence the chemistry of particle growth and composition, though. It follows, then, that adding the results from OFR experiments to that obtained by traditional environmental chambers can perhaps complement each other and provide a wider perspective on the evolution of a certain set of precursor emissions than one or the other method alone.

Research applying the concept of PAM to a variety of precursor emissions has been published since its introduction over ten years ago. OFR studies have addressed the oxidation many of the most pressing precursor emissions, including specific precursor compounds (Ahlberg *et al.*, 2017; Chen *et al.*, 2013; Mitroo *et al.*, 2018), emissions from biomass burning (Cubison *et al.*, 2011; Fortenberry *et al.*, 2018), and diesel exhaust emissions (Jathar *et al.*, 2017; Link *et al.*, 2016). In a number of studies, OFRs have been used to evaluate ambient conditions as well (Ortega *et al.*, 2016; Palm *et al.*, 2016, 2018). However, there is an apparent lack of published research regarding the use of OFRs to evaluate the oxidation of cooking-related emissions. At the time of this writing, only one published study has attempted to address emissions related to cooking. In that study, Lui

et al. (2017) used an OFR to evaluate the formation of SOA from gas-phase emissions produced by heating common cooking oils. The research presenting in this chapter will build on existing research by examining how the emissions from charbroiling hamburger patties oxidize using an OFR, how these results compare to the previous environmental chamber studies on the same emissions, and estimating the percent SOA generated by these specific meat charbroiling emissions.

3.2 Experimental Methods

3.2.1 Sampling Methodology

For this experiment, a Char-Broil Classic 280 2-Burner Propane Gas Grill was situated outside of the laboratory and used to charbroil beef hamburger patties. The two propane burners were protected by flame guards and located 10 cm from the cooking grate. Hamburgers were cooked at medium setting and the cooking surface temperature ranged between 260 and 288° C. The meat used for these tests were Kirkland Signature ¼ lb. Ground Beef Hamburger Patties and contained 22% fat as stated by the manufacturer. The hamburger patties were cooked for four minutes on each side before being removed from the grilling surface and replaced with another frozen hamburger patty. Sixteen hamburger patties were grilled one at a time over the course of approximately two hours to generate a relatively steady stream of emissions for this experiment.

The sampling line was designed to sample from the rear of the grill near the exhaust vents where a visible plume could be seen exiting the grill. The sample passed through an orifice and an ejector diluter within the first 30 cm of sample line. After two

meters, the sample passed through a vented manifold and a second ejector diluter before being diluted a third and final time at a Y-joint before entering the OFR. The compressed dilution air was set at 30 psi at the two ejector diluters and 37 psi min⁻¹ at the Y-joint. The copper injection line from sample intake outside to the OFR upstairs was 28 meters in length. See Figure 2.1 for the schematic of this dilution sampling set-up.

The OFR used for this experiment was recently built by a graduate student of the Cocker Lab Group for use at CE-CERT's Atmospheric Processes Lab. Stainless steel was used to build the OFR and the volume of the chamber is approximately 14 L (length 46 cm, diameter 20 cm). The flow rate for this reactor is 5 L min⁻¹, which results in a residence time of 170 s. Hydroxyl radicals were created by running purified dry air through a bubbler and exposing the resulting water vapor to UV radiation inside the chamber via mercury lamp (BHK, Inc., peak λ at 185 and 254 nm). The resulting hydroxyl radical exposure inside the reactor was found to be 1.33×10^{12} molecules s cm⁻³ by following the methods of Lambe *et al.* (2011). The starting concentration of benzene, used to find the hydroxyl radical exposure used here, was found to be 10.95 ppm while the VOC loading during this experiment was estimated at 3.4 ppm. The hydroxyl radical exposure used here corresponds to approximately 10 days of atmospheric oxidation, assuming an ambient hydroxyl radical concentration of 1.5×10^6 molecules cm⁻³ (Mao *et al.*, 2009). Note that the difference in the starting concentration of benzene and the experimental VOC loading may cause some variability in the above approximation. The sampling line from the OFR was connected to the APL's instruments for analysis. See figure 3.1 for a schematic of the OFR set-up used in this experiment.

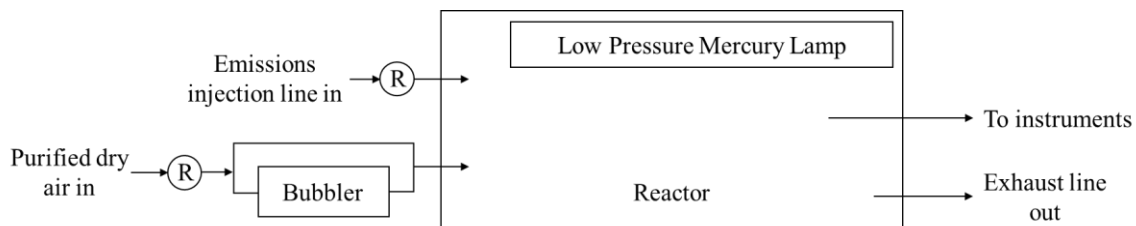


Figure 3.1. Schematic of the Oxidation Flow Reactor (OFR) used in this research. Key: R – rotameter.

3.2.2 Instrumental Analysis

A High-Resolution Time of Flight Aerosol Mass Spectrometer (HR-ToF-AMS) manufactured by Aerodyne Research Inc. was used to characterize the primary organic aerosol (POA) as it was deposited into the chamber and the secondary organic aerosol (SOA) that was formed over the course of the experiment. The voltage of the Tungsten filament was 70eV and the vaporizer temperature was set at 600°C. A commercial scanning mobility particle sizer (SMPS) was used for this experiment (TSI, Scanning Mobility Particle Sizer Spectrometer 3936 with Differential Mobility Analyzer 3081 and Ultrafine Condensation Particle Counter 3776, low flow). As with all SMPS instruments, this SMPS sizes particles based on the particle’s electric mobility and operates on the assumption that the particles being analyzed are spherical. A Kanomax Aerosol Particle Mass (APM) analyzer, assembled by the Cocker Lab Group, was used to estimate the density of the aerosol being sampled and produced in conjunction with the SMPS. Last, a Volatility Tandem Differential Mobility Analyzer (VTDMA) was used to estimate the volatility of the aerosol being sampled and produced in the OFR. The VTDMA used for these experiments was designed and assembled by the Cocker Lab Group.

3.2.3 Data Analysis

Data from the Aerodyne AMS was analyzed using Igor Pro 6.3.7.2 by Wavemetrics using the macros SQUIRREL v1.56D and PIKA v1.15D developed by the Jimenez Group at the University of Colorado, Boulder. A Microsoft Excel file created by the Cocker Lab Group was used to analyze the data obtained from the SMPS and combine this information with data obtained by the APM and VTDMA. This file was used to document the raw data as well as calculate particle mass and volume over the course of the experiment. Two MATLAB functions created by the Cocker Lab Group were used to analyze data from the APM to calculate aerosol particle density and to analyze data obtained from the VTDMA to calculate the volume fraction remaining (VFR) respectively.

Angle theta (θ) was used throughout this research to quantify the change between mass spectra obtained by the AMS (Kostenidou *et al.*, 2009). Typically, angle theta is used when spectra are nearly identical since this method is much more precise than the Pearson correlation coefficient (Pearson's r) or the coefficient of determination (R^2). Mass spectra are written as vectors for this method of analysis then compared, with $\theta = 0$ for identical spectra and $\theta = 90$ degrees for completely opposing spectra.

3.3 Results and Discussion

3.3.1 Aging in Oxidation Flow Reactor Experiment

This section discusses the data obtained by evaluating charbroiled hamburger emissions with an oxidation flow reactor (OFR) and compares these findings to those

found using the APL’s environmental chamber to evaluate the same emission source. This work builds upon the work conducted in chapter two; where the unfiltered environmental chamber experiments represented the aging of both POA and SOA generated by meat charbroiling emissions and the filtered environmental chamber experiments represented the aging of purely SOA generated by the gaseous emissions from meat charbroiling, the findings from the OFR are hypothesized to represent the extreme aging of both POA and SOA generated by meat charbroiling over an equivalent time of 1 – 2 weeks under atmospheric conditions.

The oxidative trend observed in the environmental chamber experiments continues to be observed in the results from the OFR experiment. Triangle plots and Van Krevelen diagrams, both introduced in chapter two, are the most common methods for evaluating the oxidation of atmospheric emissions. Figure 3.2 compares a representative

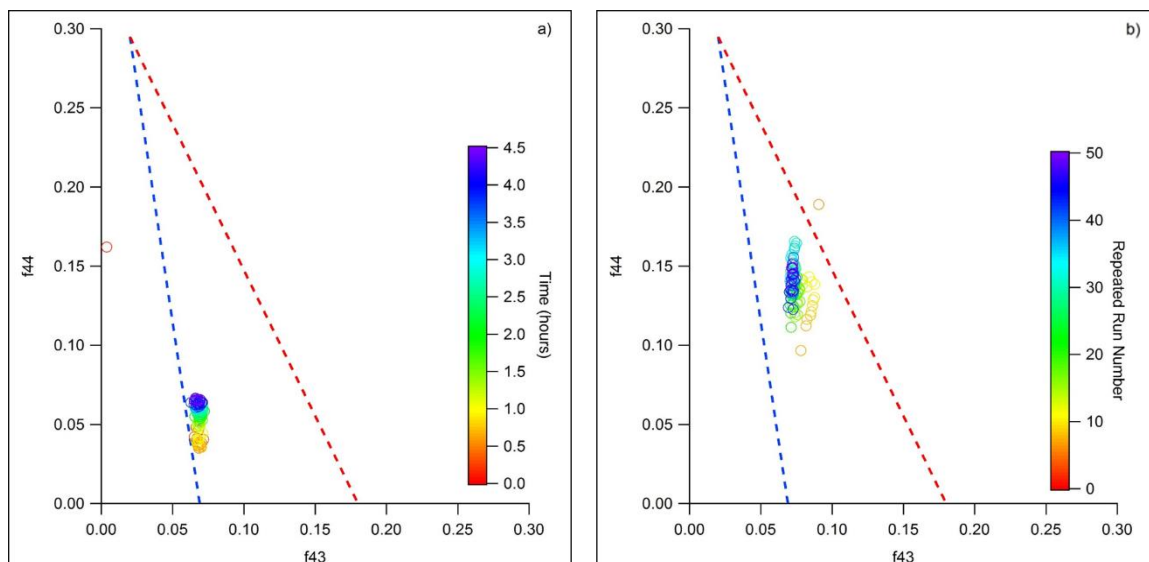


Figure 3.2. Triangle plots illustrating the oxidation of meat charbroiling emissions for a) unfiltered environmental chamber experiments and b) the OFR experiment. Figure 3.2 a) is representative of all three unfiltered environmental chamber runs and figure 3.2 b) includes approximately 50 repeated runs with the OFR. Comparing these two plots clearly illustrates the shift from less oxidized semi-volatile oxidized organic aerosol (SVOOA) at the bottom of the plot to highly oxidized low-volatile oxidized organic aerosol (LVOOA) towards the apex of the triangle.

triangle plot for the unfiltered environmental chamber experiments in figure 3.2 a) and a triangle plot showing the repeated runs from the OFR experiment in figure 3.2 b). The emissions in the unfiltered environmental chamber experiments show a clear progression of oxidation from the start to the finish in each individual experiment, although the emissions still occupy the lower portion of the plot at their most oxidized and are still considered semi-volatile oxidized organic aerosols (SVOOA). The triangle plot for the OFR experiment does not show a trend over time, as each point represents a repeated run in this figure, but the average oxidation of the meat charbroiling emissions is far greater than either the unfiltered or filtered environmental chamber experiments. The triangle plot obtained from the OFR experiment resemble low-volatile oxidized organic aerosols (LVOOA) and more closely match what is frequently obtained from ambient measurements.

Figure 3.3 compares a representative Van Krevelen diagram for an unfiltered environmental chamber experiment in figure 3.3 a) and a Van Krevelen diagram showing the repeated runs from the OFR experiment in figure 3.3 b). It is important to note that the apparent slope of the data in figure 3.3 b) should be disregarded, as this figure shows approximately 50, 170 s repeated runs from the OFR experiment. Despite the lack of a useable slope in figure 3.3 b), figures 3.5 a) and b) together still illustrates the continued oxidation of the emissions found in the unfiltered environmental chamber experiments. The nearly zero slope of the trend line in figure 3.3 a) indicates that the oxidative pathway for the aging of meat charbroiling emissions involves the addition of alcohol and/or peroxide groups, since oxygen atoms are being added while little to no hydrogen

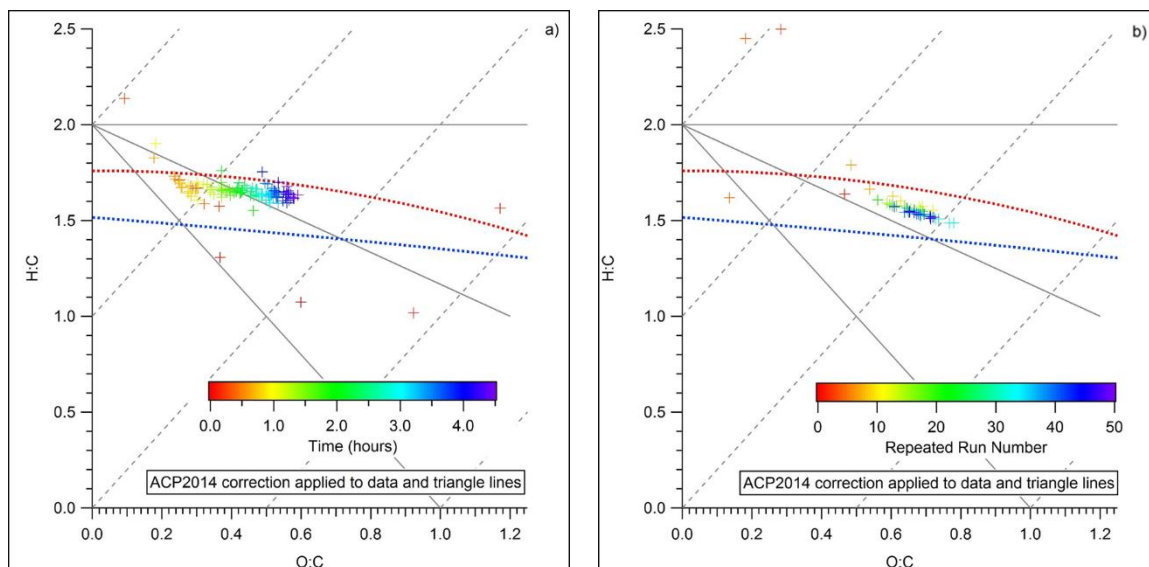


Figure 3.3. Van Krevelen diagrams illustrating the oxidation of meat charbroiling emissions for a) unfiltered environmental chamber experiments and b) the OFR experiment. Figure 3.3 a) is representative of all three unfiltered environmental chamber runs and figure 3.3 b) includes approximately 50 repeated runs with the OFR. The apparent slope of figure 3.3 b) should not be considered as each point represents a repeated run, however, clear oxidation can be seen from figure 3.3 a) to b).

atoms are being lost through the aging process. While the perceived slope information cannot be used, a lower H:C ratio and a greater O:C ratio can be observed in figure 3.3 b). This potentially suggests that as the emissions continue to age past what is observed in the environmental chamber experiments, the oxidative pathway may shift from one where oxygen atoms are gained without much loss of hydrogen atoms to one where oxygen atoms are gained while seeing a greater loss of hydrogen atoms. Alternatively, these early results might indicate that the mechanism of oxidation is simply different than that seen in environmental chambers for these emissions.

3.3.2 Character Change in Oxidation Flow Reactor Experiment

The normalized representative mass spectra of the organic component of meat charbroiling emissions for these three different types of experiments can be seen in figure

3.4, with a) illustrating the composition at the beginning of an unfiltered environmental chamber experiment, b) illustrating the composition at the end of an unfiltered environmental chamber experiment, c) illustrating the average composition for the OFR experiment, and d) illustrating the composition at the end of a filtered environmental chamber experiment. Figure 3.4 c) is the average of approximately 50 runs with a residence time of 170 s each while the other three spectra are representative of three environmental chambers repeats for each experiment type. The labelled peaks in figure 3.4 were marked as important cooking-related organic aerosols (COA) based on previous published literature as discussed in chapter two.

The trends observed in the mass spectra from the previous chapter continue to be seen in the OFR results. Fragments m/z 28 and 44 continue to increase from figure 3.4 a)

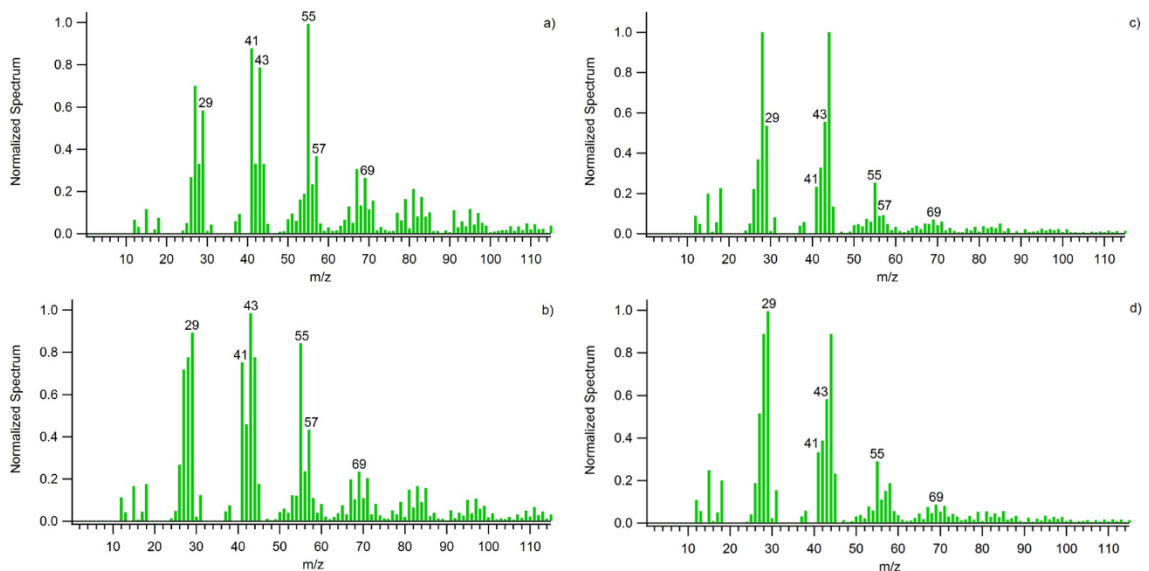


Figure 3.4. Normalized representative mass spectra for the average of a) the beginning of an unfiltered environmental chamber experiment, b) the end of an unfiltered environmental chamber experiment, c) the average from the OFR experiment, and d) the end of a filtered environmental chamber experiment. Figure 3.4 c) represents approximately 50 repeated runs, with each run having a residence time of 170 s. Peaks of interest are labelled in accordance with the cooking-related organic aerosol (COA) mass spectra markers that were selected in chapter two.

to c), clearly becoming the dominating peaks in the OFR spectrum. Likewise, peaks m/z 41, 43, 55, 57, and 69 continue to decrease from figure 3.4 a) to c). Unexpectedly, fragments m/z 29 and 43 decrease dramatically from the unfiltered environmental chamber spectra in figure 3.4 a) and b), where the two fragments seemed to be increasing, to the OFR spectrum in figure 3.4 c). A closer inspection of the high-resolution (HR) data from the aerosol mass spectrometer (AMS) shows a continued shift towards the oxygenated component of each of the three fragments inspected. The specific results can be found in table 3.1.

Angle theta was again calculated to find a quantitative difference between the average mass spectra obtained from the environmental chamber experiments and the average mass spectrum from the OFR experiment. The change in theta between the

Experiment Type	m/z 29: $\text{CHO}^+/\text{C}_2\text{H}_5^+$	m/z 43: $\text{C}_2\text{H}_3\text{O}^+/\text{C}_3\text{H}_7^+$	m/z 55: $\text{C}_3\text{H}_3\text{O}^+/\text{C}_4\text{H}_7^+$
Unfiltered at Start, Environmental (POA)	1.80	1.29	1.05
Unfiltered at End, Environmental (POA and SOA)	2.36	1.38	1.10
Unfiltered Average, OFR (POA and SOA)	14.7	4.28	2.89
Filtered Average, Environmental (SOA)	19.8	3.68	1.22

Table 3.1. Table building off the information presented in chapter two with table 2.1, illustrating how the composition of meat charbroiling emissions for a sample of prominent fragments in these experiments became more oxidized over time. The numbers presented for the unfiltered and filtered environmental chamber experiments are an average of three chamber runs each. The numbers presented for the OFR experiments represent an average of approximately 50 runs with a residence time of 170 s each. These values emphasize the importance of evaluating the high-resolution data along with the mass spectra for meat charbroiling experiments.

spectrum from the beginning of the unfiltered environmental chamber, figure 3.4 a), and the spectrum from the OFR experiment, figure 3.4 c), was found to be 46.2 ± 0.9 degrees. The change in angle theta from the end of the filtered environmental chamber spectrum, figure 3.4 d), and the OFR spectrum, figure 3.4 c), is 19.3 ± 4.4 degrees. This result makes sense, as it would be expected that the highly oxidized OFR spectrum would more closely resemble the filtered gas-only emissions obtained in the environmental chamber since the filtered chamber experiments were said to represent the SOA-only emissions and the OFR quickly oxidizes primary emissions to their most oxidized SOA predominant state. Even then, an angle theta of 19.3 ± 4.4 degrees shows considerable divergence between the two spectra being compared, representing an R^2 value between 0.7 and 0.8.

Figure 3.5 shows the average mass spectra, including inorganic ions along with the organic ions previously addressed, for each of these experiment types. This comparison provides some interesting insight as well. Figure 3.5 a) shows a representative average mass spectrum from the beginning of an unfiltered environmental chamber experiment, which represents primary meat charbroiling emissions, and figure 3.5 b) shows a representative average mass spectrum from the end of the same unfiltered environmental chamber experiment, which represents aged POA and SOA generated by meat charbroiling. The results from the OFR experiment add to these spectra, originally presented in chapter two, and can be seen in figure 3.5 c). The OFR experiment represents the highly aged POA and SOA emissions from meat charbroiling. Finally, figure 3.5 d) presents a representative spectrum from the end of a filtered environmental

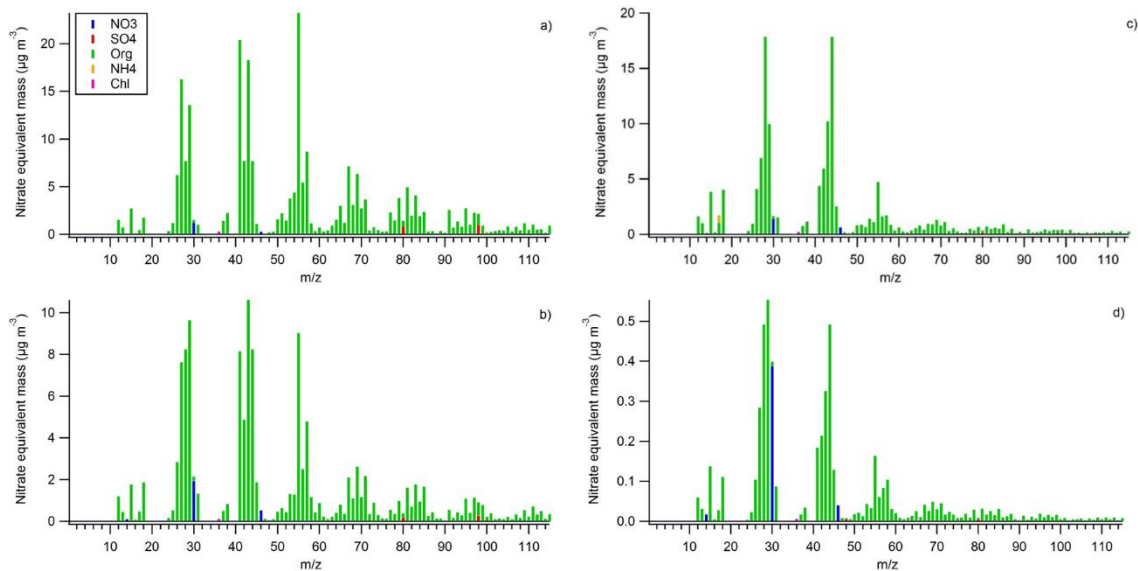


Figure 3.5. Representative average mass spectra of meat charbroiling emissions taken from a) the beginning of an unfiltered environmental chamber experiment, b) the end of an unfiltered environmental chamber experiment, c) the average from the OFR experiment, and d) the end of a filtered environmental chamber experiment. Figure 3.5 c) represents approximately 50 repeated runs, with each run having a residence time of 170 s. An increase in NO_3 compounds and a decrease in SO_4 compounds can be observed between the unfiltered and filtered chamber experiments, figure 3.5 a) and d), though overall the non-organic ions do not have a significant signature in the OFR chamber experiments, figure 3.5 c).

chamber experiment and represents the SOA-only emissions from meat charbroiling. The addition of the spectrum from the OFR experiment does not match well with the hypothesis presented in chapter two regarding figure 3.5 a), b), and d), which suggested that aged meat charbroiling emissions showed an increase in NO_3 compounds and a decrease in SO_4 compounds. Instead, the average mass spectrum obtained from the OFR experiment more closely resembles spectra found from the beginning of the unfiltered environmental chamber experiments. This suggests that the meat charbroiling emissions may not change appreciable in ionic composition beyond the obvious change in organic ion character shown in figure 3.4. A possible explanation for this may be the low starting mass concentration present in the filtered environmental chamber experiments producing misleading results regarding the significance of the changing NO_3 ion fragments.

3.3.3 Percent Secondary Organic Aerosol Production

A linear combination of variables was used with data obtained from both the environmental chamber and OFR to estimate the percent secondary organic aerosol (%SOA) produced by charbroiled meat emissions. For this calculation, mass spectra from the six environmental chamber experiments were normalized with respect to m/z 44 and values for m/z fragments 29, 43, 44, and 55 were recorded. The mass spectrum obtained from the OFR experiment, averaging approximately 50 repeated runs, was also normalized with respect to m/z 44 and the same four fragment values were recorded. Table 3.2 shows the average values used for this calculation.

The following equation was used as the starting point to calculate the %SOA using the linear combination of variables method:

$$\sum_n [(an_F + bn_{UF}) - n_{OFR}]^2, \quad (3.1)$$

where

n is the corresponding average values for m/z fragments 29, 43, 44, and 55,

F denotes the filtered environmental chamber average value for n ,

UF denotes the unfiltered environmental chamber average value for n ,

OFR denotes the OFR average value for n , and

a and b are unknown coefficients, with $b = 1 - a$.

The corresponding values for n_F , n_{UF} , and n_{OFR} were substituted into equation 3.1, then the equation was simplified. Next, the derivative of equation 3.1 was taken to find the minimum and the equation was set to zero to solve for a .

MS Fragment	Unfiltered Average	Filtered Average	PAM Average
m/z 29	1.61	1.17	0.53
m/z 43	2.19	0.64	0.56
m/z 44	1.00	1.00	1.00
m/z 55	2.81	0.31	0.25

Table 3.2. Average values for chosen m/z fragments from mass spectra normalized with respect to m/z 44 for use with equation 3.1 to estimate %SOA. Unfiltered and filtered averages are based on three repeated runs each while the OFR averages are based on approximately 50 repeated runs, each with an emission residence time of 170 seconds.

Last, the following equation was used to calculate %SOA:

$$\%SOA = \frac{b}{b + a} \times 100, \quad (3.2)$$

where $a = 0.43$ and $b = 0.57$.

Using this method, the %SOA created by charbroiling hamburger emissions was calculated to equal 57%. This means that for every 1 unit of primary pollution created by hamburger charbroiling, 0.57 units of SOA is created in the atmosphere. This value is significantly higher than anticipated and has tremendous implications for air quality in areas where primary pollution from commercial cooking sources are already significant.

3.4 Summary

The addition of the OFR results continues to affirm the hypothesis that long-chain alkyl backbones make up the majority of meat charbroiling emissions and that these emissions degrade readily into smaller common molecules when exposed to atmospheric conditions. Furthermore, the average mass spectrum obtained from the OFR experiment shown in figure 3.4 c) further illustrates the diverse signature from cooking organic

aerosol, specifically those from meat charbroiling, can radically change when exposed to atmospheric conditions. Angle theta was calculated to quantitatively compare the spectra shown in figure 3.4, finding that the difference between the OFR results and the filtered results to be $19.3 \pm 4.4^\circ$ and the difference between the OFR results and the unfiltered results to be $46.2 \pm 0.9^\circ$. This result makes sense, as one would expect that the results from the highly oxidized OFR are more closely related to the filtered experiments, which are hypothesized to represent purely the SOA generated by meat charbroiling emissions. Figure 3.5 shows that while the organic character of meat charbroiling emissions changes significantly, the inorganic portion appears more stable.

HR data continues to show a shift towards a more oxygenated composition, as can be seen in table 3.1. Figures 3.2 b) and 3.3 b) respectively show the triangle plot and the Van Krevelen diagram for the OFR results. In figure 3.2, the hamburger charbroiling emissions from the OFR experiment are clearly more oxidized and more ambient-like than the unfiltered environmental chamber results. Figure 3.3 shows an increase in O:C ratio and a slight decrease in H:C ratio for the OFR results compared to the unfiltered environmental chamber results. This may suggest that the oxidative pathway may even be changing as the emissions age, however another possibility is that the emissions are aging through a different oxidative pathway entirely in the OFR. Not enough data was obtained on this particular point to make a definitive conclusion. Overall, this information regarding the oxidation of meat charbroiling emissions does clearly show that these emissions show SOA forming potential under atmospheric conditions and oxidize significantly over time.

Last, the %SOA production of meat charbroiling emissions were calculated using a linear combination of variables and found to be 57%. This means that for one unit of primary meat charbroiling emissions released into the atmosphere, 0.57 units of SOA is produced. This value is significantly higher than any other attempt at estimating the secondary contribution of commercial cooking emissions has provided to date. More work needs to be conducted in order to find the precise %SOA produced by this emissions source, as limited OFR experiments were conducted during this research due to time constraints. Specifically, it is suggested that future research to vary the intensity of the hydroxyl radical exposure in the OFR in order to find SOA fractions at different hydroxyl radical loadings. Regardless, these initial finding has tremendous implications for regions that already have a significant impact on air quality from primary commercial cooking emissions.

3.5 References

- Ahlberg, E., Falk, J., Eriksson, A., Holst, T., Brune, W. H., Kristensson, A., ... & Svenningsson, B. (2017). Secondary organic aerosol from VOC mixtures in an oxidation flow reactor. *Atmospheric environment*, 161, 210-220.
- Bruns, E. A., El Haddad, I., Keller, A., Klein, F., Kumar, N. K., Pieber, S. M., ... & Prévôt, A. S. H. (2015). Inter-comparison of laboratory smog chamber and flow reactor systems on organic aerosol yield and composition. *Atmospheric Measurement Techniques*, 8(6), 2315-2332.
- Chacon-Madrid, H. J., & Donahue, N. M. (2011). Fragmentation vs. functionalization: chemical aging and organic aerosol formation. *Atmospheric Chemistry and Physics*, 11(20), 10553-10563.
- Chen, S., Brune, W. H., Lambe, A. T., Davidovits, P., & Onasch, T. B. (2013). Modeling organic aerosol from the oxidation of α -pinene in a Potential Aerosol Mass (PAM) chamber. *Atmospheric Chemistry and Physics*, 13(9), 5017-5031.
- Cocker, D. R., Flagan, R. C., & Seinfeld, J. H. (2001). State-of-the-art chamber facility for studying atmospheric aerosol chemistry. *Environmental science & technology*, 35(12), 2594-2601.
- Cubison, M. J., Ortega, A. M., Hayes, P. L., Farmer, D. K., Day, D., Lechner, M. J., ... & Fuelberg, H. E. (2011). Effects of aging on organic aerosol from open biomass burning smoke in aircraft and laboratory studies. *Atmospheric Chemistry and Physics*, 11(23), 12049-12064.
- Fortenberry, C. F., Walker, M. J., Zhang, Y., Mitroo, D., Brune, W. H., & Williams, B. J. (2018). Bulk and molecular-level characterization of laboratory-aged biomass burning organic aerosol from oak leaf and heartwood fuels. *Atmospheric Chemistry and Physics*, 18(3), 2199-2224.
- Jathar, S. H., Friedman, B., Galang, A. A., Link, M. F., Brophy, P., Volckens, J., ... & Farmer, D. K. (2017). Linking load, fuel, and emission controls to photochemical production of secondary organic aerosol from a diesel engine. *Environmental science & technology*, 51(3), 1377-1386.
- Kang, E., Root, M. J., Toohey, D. W., & Brune, W. H. (2007). Introducing the concept of potential aerosol mass (PAM). *Atmospheric Chemistry and Physics*, 7(22), 5727-5744.
- Kang, E., Toohey, D. W., & Brune, W. H. (2011). Dependence of SOA oxidation on organic aerosol mass concentration and OH exposure: experimental PAM chamber studies. *Atmospheric Chemistry and Physics*, 11(4), 1837-1852.

- Kostenidou, E., Lee, B. H., Engelhart, G. J., Pierce, J. R., & Pandis, S. N. (2009). Mass spectra deconvolution of low, medium, and high volatility biogenic secondary organic aerosol. *Environmental science & technology*, 43(13), 4884-4889.
- Kroll, J. H., Smith, J. D., Che, D. L., Kessler, S. H., Worsnop, D. R., & Wilson, K. R. (2009). Measurement of fragmentation and functionalization pathways in the heterogeneous oxidation of oxidized organic aerosol. *Physical Chemistry Chemical Physics*, 11(36), 8005-8014.
- Lambe, A. T., Ahern, A. T., Williams, L. R., Slowik, J. G., Wong, J. P. S., Abbatt, J. P. D., ... & Worsnop, D. R. (2011). Characterization of aerosol photooxidation flow reactors: heterogeneous oxidation, secondary organic aerosol formation and cloud condensation nuclei activity measurements. *Atmospheric Measurement Techniques*, 4(3), 445-461.
- Lambe, A. T., Onasch, T. B., Croasdale, D. R., Wright, J. P., Martin, A. T., Franklin, J. P., ... & Worsnop, D. R. (2012). Transitions from functionalization to fragmentation reactions of laboratory secondary organic aerosol (SOA) generated from the OH oxidation of alkane precursors. *Environmental science & technology*, 46(10), 5430-5437.
- Lambe, A. T., Chhabra, P. S., Onasch, T. B., Brune, W. H., Hunter, J. F., Kroll, J. H., ... & Kolb, C. E. (2015). Effect of oxidant concentration, exposure time, and seed particles on secondary organic aerosol chemical composition and yield. *Atmospheric Chemistry and Physics*, 15(6), 3063-3075.
- Link, M. F., Friedman, B., Fulgham, R., Brophy, P., Galang, A., Jathar, S. H., ... & Farmer, D. K. (2016). Photochemical processing of diesel fuel emissions as a large secondary source of isocyanic acid (HNCO). *Geophysical Research Letters*, 43(8), 4033-4041.
- Liu, T., Li, Z., Chan, M., & Chan, C. K. (2017). Formation of secondary organic aerosols from gas-phase emissions of heated cooking oils. *Atmospheric Chemistry and Physics*, 17(12), 7333-7344.
- Mao, J., Ren, X., Brune, W. H., Olson, J. R., Crawford, J. H., Fried, A., ... & Blake, D. R. (2009). Airborne measurement of OH reactivity during INTEX-B. *Atmospheric Chemistry and Physics*, 9(1), 163-173.
- Matsunaga, A., & Ziemann, P. J. (2010). Gas-wall partitioning of organic compounds in a Teflon film chamber and potential effects on reaction product and aerosol yield measurements. *Aerosol Science and Technology*, 44(10), 881-892.

- Mitroo, D., Wu, J., Colletti, P. F., Lee, S. S., Walker, M. J., Brune, W. H., ... & Fortner, J. D. (2018). Atmospheric Reactivity of Fullerene (C60) Aerosols. *ACS Earth and Space Chemistry*, 2(2), 95-102.
- Ortega, A. M., Hayes, P. L., Peng, Z., Palm, B. B., Hu, W., Day, D. A., ... & Warneke, C. (2016). Real-time measurements of secondary organic aerosol formation and aging from ambient air in an oxidation flow reactor in the Los Angeles area. *Atmospheric Chemistry and Physics*, 16(11), 7411-7433.
- Palm, B. B., Campuzano-Jost, P., Ortega, A. M., Day, D. A., Kaser, L., Jud, W., ... & Kroll, J. H. (2016). In situ secondary organic aerosol formation from ambient pine forest air using an oxidation flow reactor. *Atmospheric Chemistry and Physics*, 16(5), 2943-2970.
- Palm, B. B., Sá, S. S. D., Day, D. A., Campuzano-Jost, P., Hu, W., Seco, R., ... & Brito, J. (2018). Secondary organic aerosol formation from ambient air in an oxidation flow reactor in central Amazonia. *Atmospheric Chemistry and Physics*, 18(1), 467-493.

Chapter 4

Conclusion

Primary fine particulate matter (PM_{2.5}) emissions from commercial cooking is now the single greatest source of PM_{2.5} emissions in the South Coast Air Basin, even exceeding the primary PM_{2.5} emissions produced by heavy-duty diesel trucks and passenger cars. Within the commercial cooking category, the underfired charbroiling of meat has previously been identified as the cooking method responsible for contributing the most to these primary commercial cooking emissions. Studies have consistently found increasing emissions with increasing fat content of the meat being cooked, and researchers suspect that underfired charbroilers and fatty meats make such a potent combination due to the charbroiler's open flame and high cooking temperatures. This particular set-up allows for liquid fat droplets released from the cooking meat to drip down into the open flame where the fat droplets become volatilized and entrained in the exhaust fume. Previous research has also found that charbroiling emissions produce the greatest concentration of volatile organic compounds (VOCs) compared to other cooking methods, and that the oxidation of VOCs evaporated from primary particulate matter (PM) can produce significant secondary organic aerosol (SOA). Additionally, charbroiling emissions have been shown to have a high ozone forming potential and other studies have estimated commercial cooking emissions to contribute 19-35% of regional SOA using programs intended to model transportation emissions. With the above research considered, commercial cooking emissions has a substantial potential to

contribute tremendously to SOA production in regions where the primary emissions for commercial cooking are already significant.

The research for this thesis was conducted with the intent to provide insight into the secondary impact of meat charbroiling emissions, a topic that has not been well-explored by previous research endeavors. Chamber experiments were conducted inside the Atmospheric Process Laboratory (APL) at the College of Engineering – Center for Environmental Research and Technology (CE-CERT) in Riverside, CA, between July 2017 and May 2018. Experiments were conducted to evaluate the evolution of meat charbroiling emissions over time under atmospheric condition with a 37.5 m³ environmental chamber and a 14 L oxidation flow reactor (OFR). Hydrogen peroxide was injected as a source of hydroxyl radicals for the environmental chamber experiments, and the contents of the environmental chamber was exposed to ultraviolet radiation (UV) provided by black lights to simulated atmospheric-like conditions. For half of the environmental chamber experiments, a Teflon filter was used prior to emission injection into the chamber to study the gas-only emissions created by meat charbroiling. For the OFR, hydroxyl radicals were created by running purified dry air through a bubbler and exposing the resulting water vapor to UV radiation inside the chamber via low pressure mercury lamp. The resulting hydroxyl radical exposure was 1.33×10^{12} molecules s cm⁻³, corresponding to approximately 10 days of atmospheric oxidation assuming an ambient hydroxyl radical concentration of 1.5×10^6 molecules cm⁻³. The flow rate for the OFR was 5 L min⁻¹ and the residence time of was 170 s.

From data obtained at the beginning of unfiltered environmental chamber experiments before the black lights were turned on and before injection of hydrogen peroxide, representing the primary organic aerosol (POA) produced by meat charbroiling, it was concluded that the mass spectra collected under these circumstances deviated considerably from what was previously considered a standard for fatty hamburger charbroiling emissions. Furthermore, the character of these emissions changed significantly over the duration of the environmental chamber experiments and between the separate experiment types. The prominent peaks in the unfiltered environmental chamber experiments, which represent the aging of both POA and SOA produced by meat charbroiling, shifted from m/z 27, 41, 43, and 55 to clearly favor m/z 29, and 43. For the filtered environmental chamber experiments, which represent the aging of purely SOA emissions from meat charbroiling, the prominent peaks shifted from m/z 43 and 55 to m/z 29 and 44. The OFR experiment, representing the extreme aging of POA and SOA emissions from meat charbroiling, yielded spectra that plainly favored m/z 28 and 44. Additionally, high resolution (HR) data from the AMS was evaluated for select peaks of interest in these experiments and a consistent trend was observed in the ratio of hydrocarbon ions and oxidized ions that make up these m/z fragments. The ratio between these ions shifted over time and across the different experiment types to clearly favor the oxidized portion of the m/z signal, highlighting the importance to consider HR AMS data when trying to understand the changing character of meat charbroiling emissions.

An attempt to quantify the changes between spectra through the use of angle theta was made. From beginning to end, the unfiltered environmental chamber experiments

changed by an angle θ of 19.3 ± 2.6 degrees and the filtered environmental chamber experiments changed by 51.8 ± 3.5 degrees. This suggests that the aerosol formed from the gas-only portion of meat charbroiling emissions are far more reactive under atmospheric conditions than those formed alongside the primary PM emissions. The difference in angle θ between the start of the unfiltered environmental chamber experiments and the average obtained by the OFR experiment was 46.2 ± 0.9 degrees and the difference between the end of the filtered environmental chamber experiments and the average obtained by the OFR experiment was 19.3 ± 4.4 degrees. This suggests that the extremely aged POA and SOA emissions in the OFR experiment show more similarities to the aged SOA-only emissions from the filtered environmental chamber experiments than the moderately aged POA and SOA emissions from the unfiltered environmental chamber experiments. Furthermore, it confirms the changing character of these emissions and the need to consider how these emissions change in the atmosphere when attempts to trace or model this emission source are made.

Oxidative information from these experiments were also gathered and analyzed, mainly through the use of triangle plots and Van Krevelen diagrams. The triangle plot and the Van Krevelen diagram for the unfiltered experiments show a clear increase in oxidation over time. Additionally, the trend line through the data in the unfiltered chamber experiments' Van Krevelen diagrams are nearly zero, suggesting that the oxidative pathway for the ageing of these emissions involve the addition of alcohol and/or peroxide groups. Van Krevelen diagrams from the filtered environmental chamber experiments and the OFR experiments do not provide a useable trend line due to the

nature of the experiments, but the filtered environmental chamber experiments show an increase in O:C ratio and the OFR experiments shows further increase in O:C and a slight decrease in H:C ratios. The triangle plots for the unfiltered environmental chamber experiments, the filtered environmental chamber experiments, and the OFR experiments show progressive increase in oxidation. The emissions in the unfiltered environmental chamber experiments are located near the base of the triangle, the area associated in literature with environmental chamber measurements and semi-volatile oxidized organic aerosol (SVOOA). The OFR results, however, are located closer to the apex of the triangle, the area more closely associated with ambient atmospheric measurements and low-volatile oxidized organic aerosol (LVOOA). These results confirm the SOA forming potential of these emissions under atmospheric conditions.

Finally, the percent SOA production from meat charbroiling emissions was estimated using two different methods for this research. The first method utilized results from the unfiltered and filtered environmental chamber experiments and a method originally used to evaluate diesel emissions. This method found that the unfiltered environmental chamber experiments consisted of $13 \pm 5.6\%$ SOA after one hour and $24 \pm 6.7\%$ SOA after four hours with the chamber's black lights on. The filtered environmental chamber experiments remained more constant at a much higher percent SOA, yielding $90 \pm 9.8\%$ SOA on average. The results from this calculation are visually represented in figure 2.7 where they are plotted against time. These results help confirm the hypothesis that the unfiltered environmental chamber experiments represent the POA and SOA generated by meat charbroiling emissions while the filtered environmental

chamber experiments represent only the SOA generated by meat charbroiling. The second method of estimating the percent SOA production of meat charbroiling emissions utilized a linear combination of variables and data from both of the environmental chamber and OFR experiments. This method estimated the percent SOA to be 57%. This means that for every one unit of primary meat charbroiling emissions released into the atmosphere, 0.57 units of SOA is produced.

The results for the percent SOA generation by meat charbroiling emissions are significantly higher than any other attempt at estimating the secondary contribution of commercial cooking emissions has provided to date. More work needs to be conducted to find the precise percent SOA produced by this emissions source, as limited OFR experiments were conducted during this research due to time constraints. Specifically, it is suggested that future research to vary the intensity of the hydroxyl radical exposure in the OFR in order to find SOA fractions at different hydroxyl radical loadings. Nonetheless, these early findings have tremendous implications since they confirm that the secondary impact of commercial cooking emissions, already responsible for contributing the most primary PM_{2.5} emissions in the South Coast Air Basin, has been exceptionally underestimated.